Symmetry analysis of holes localized on a skyrmion in a doped antiferromagnet

N. D. Vlasii,[1] C. P. Hofmann,[2] F.-J. Jiang,[3,*] and U.-J. Wiese[4]

[1]*Physics Department, Taras Shevchenko National University of Kyiv, 64 Volodymyrska str., Kyiv 01601, Ukraine*
[2]*Facultad de Ciencias, Universidad de Colima, Bernal Diaz del Castillo 340, Colima C.P. 28045, Mexico*
[3]*Department of Physics, National Taiwan Normal University, 88 Sec. 4, Ting-Chou Rd., Taipei 116, Taiwan*
[4]*Albert Einstein Center for Fundamental Physics, Institute for Theoretical Physics, Bern University, Sidlerstrasse 5, CH-3012 Bern, Switzerland*

(Received 26 May 2012; published 8 October 2012)

We use the low-energy effective field theory for holes coupled to the staggered magnetization in order to investigate the localization of holes on a skyrmion in a square lattice antiferromagnet. When two holes get localized on the same skyrmion, they form a bound state. The quantum numbers of the bound state are determined by the quantization of the collective modes of the skyrmion. Remarkably, for p-wave states, the quantum numbers are the same as those of a hole pair bound by one-magnon exchange. Two holes localized on a skyrmion with winding number $n = 1$ or 2 may have s- or d-wave symmetry as well. Possible relations with preformed Cooper pairs of high-temperature superconductors are discussed.

DOI: 10.1103/PhysRevB.86.155113 PACS number(s): 71.10.Fd, 71.27.+a

I. INTRODUCTION

In the cuprates, high-temperature superconductivity is separated from antiferromagnetism by a pseudogap regime. It has been conjectured that the relevant low-energy degrees of freedom in the pseudogap regime are responsible for superconductivity as well. Reliably identifying those degrees of freedom by theoretical investigations is a highly nontrivial task because unbiased first-principles analytic or numerical calculations in microscopic systems such as the Hubbard or t-J model are presently out of reach. In lightly doped antiferromagnets, on the other hand, the situation is more favorable. First of all, precise numerical simulations of undoped antiferromagnets[1–4](such as the Heisenberg model) are possible with the loop-cluster algorithm,[5] and individual doped holes can also be simulated reliably.[6,7] Second, the low-energy dynamics of lightly doped antiferromagnets can be described with a systematic effective field theory for magnons and holes. The pure magnon effective field theory has been developed in Refs. 8–11 and is completely analogous to chiral perturbation theory for the Goldstone pions in QCD.[12] In the past few years, the systematic effective theory for magnons and doped holes has been constructed[13,14] in complete analogy to baryon chiral perturbation theory: the effective theory for pions and nucleons.[15–18] In contrast to previous attempts to construct effective theories for magnons and holes in a square lattice antiferromagnet,[19–23] the construction of Ref. 14 is based on a systematic symmetry analysis and provides a complete set of all terms contributing to the effective action at leading and subleading order. As a result, the predictions of the effective theory are exact, order by order, in a systematic derivative expansion. In particular, the low-energy physics of any lightly doped antiferromagnet is described quantitatively once some low-energy parameters (such as the spin stiffness or the spin-wave velocity of the underlying microscopic system) have been fixed either by experiment or by numerical simulations. The effective theory has been used in systematic studies of magnon-mediated two-hole bound states[24] and of spiral phases.[25] Earlier (but somewhat less systematic) studies had been presented in Refs. 23, 26, and 27. Systematic effective field theories have also been constructed for antiferromagnets on a honeycomb lattice[28,29] as well as for lightly electron-doped antiferromagnets.[30]

Unfortunately, before one enters the high-temperature superconductor or even just the pseudogap regime, both antiferromagetism and the systematic effective theory that describes it break down. While one might expect that one can hence not learn anything about high-temperature superconductivity or the pseudogap regime from the effective theory, the situation may not be entirely hopeless. In particular, the effective theory still contains information about what objects may form when the theory is about to break down. In this way, we can identify new candidate low-energy degrees of freedom for which another effective theory with an extended validity range can be constructed. In this paper, we do not yet attempt to construct an effective field theory for the pseudogap regime. Instead, we concentrate on the identification of new low-energy objects that may form when antiferromagnetism is about to break down.

When antiferromagnetism is weakened, the spin stiffness ρ_s is reduced. In particular, if antiferromagnetism is ultimately destroyed in a second-order phase transition, ρ_s vanishes at the transition. A small value of ρ_s favors topological excitations in the staggered magnetization: the order parameter for antiferromagnetism. In $(2+1)$ dimensions, the topological excitations of the staggered magnetization vector are skyrmions which carry a topologically conserved winding number $n \in \Pi_2[S^2] = \mathbb{Z}$ in the second homotopy group of the order parameter manifold S^2. The coset space $S^2 = \mathrm{SU}(2)_s/\mathrm{U}(1)_s$ arises because in an antiferromagnet the $\mathrm{SU}(2)_s$ spin symmetry is spontaneously broken down to the subgroup $\mathrm{U}(1)_s$. The possible role of skyrmions as relevant excitations in quantum antiferromagnets has been discussed in several publications.[31–45] Other topological objects, including vortices and merons, have also been investigated in this context.[46–49] Haldane was first to realize that skyrmions in an antiferromagnet are associated with a geometric phase.[31] When skyrmions proliferate, antiferromagnetic order is destroyed. Read and Sachdev showed that, on a square lattice, the skyrmion's geometric phase then implies a competing valence bond solid order with fourfold degeneracy.[32] The interplay of geometric phases and competing orders has been discussed in detail in Ref. 43. The suppression of skyrmions has been related to unconventional deconfined quantum critical points.[38,39] It has also been argued that a hole localized near a dopant stabilizes a skyrmion texture in the staggered magnetization.[33–37] The analogies between pions in QCD and magnons in ferromagnets and antiferromagnets have been investigated in detail in Refs. 40 and 41. In particular, it was argued that skyrmions endowed with fermion number 2 may act as preformed Cooper pairs of high-temperature superconductivity. Experimental evidence for skyrmions in the lightly doped insulating antiferromagnet $La_2Cu_{1-x}Li_xO_4$ in an external magnetic field has been reported in Ref. 44. Furthermore, the possible role of skyrmions for the superconductivity of Fe based pnictides and chalcogenides has been discussed in Ref. 45. In this paper, we investigate the localization of holes on a skyrmion using the low-energy effective theory for lightly hole-doped antiferromagnets on a square lattice. In particular, we carefully quantize the skyrmion's collective modes, which allows us to unambiguously determine the quantum numbers of single holes as well as hole pairs localized on a skyrmion.

At the classical level, the mass of a skyrmion is given by $4\pi\rho_s$. When ρ_s becomes small, these excitations hence become energetically favorable. Skyrmions are beyond the reach of the systematic derivative expansion of the low-energy effective theory for magnons and holes. Indeed, when skyrmions become relevant low-energy degrees of freedom, antiferromagnetism as well as the effective theory that describes it are about to break down. Still, the effective theory correctly describes the way in which holes couple to a skyrmion excitation in the staggered magnetization order parameter. In particular, holes may get localized on a skyrmion. When two holes get localized on the same skyrmion, they form a bound state which may represent a relevant low-energy degree of freedom even when antiferromagnetism gives way to the pseudogap phase. In particular, such bound states are a potential candidate for preformed pairs, the condensation of which may ultimately lead to high-temperature superconductivity. In order to decide whether this is a viable scenario, in this paper we investigate the symmetry properties of skyrmion-hole bound states in great detail. We find that the p-wave states of two holes localized on a skyrmion with winding number $n = 1$ transform exactly like the two-hole states weakly bound by one-magnon exchange. Two holes localized on a skyrmion may also have s- or d-wave symmetry. Which of these states is energetically most favorable depends on the details of the dynamics, and will remain a subject for future investigations.

The rest of the paper is organized as follows. In Sec. II, the effective theory for the staggered magnetization order parameter is introduced and skyrmions are discussed as classical solutions. The Hopf term is introduced and the collective modes of a rotating skyrmion are then quantized. In Sec. III, doped holes are added to the effective theory. In Sec. IV, states of single holes as well as a pair of holes (residing in two different hole pockets) localized on a static or rotating skyrmion are constructed and their symmetry properties are investigated. Possible relations to the mechanism responsible for high-temperature superconductivity are also discussed. Section V contains our conclusions. Finally, the case of two holes residing in the same hole pocket is investigated in the Appendix. A reader who is only interested in the main results of our study may skip Sec. II C as well as Sec. III.

II. SKYRMIONS IN THE EFFECTIVE THEORY FOR THE STAGGERED MAGNETIZATION

In this section, we discuss the collective mode quantization of skyrmions in the low-energy effective theory for antiferromagnetic magnons.

A. Effective action and its symmetries

Magnons are the Goldstone bosons of a spontaneously broken spin symmetry $SU(2)_s$ with an unbroken subgroup $U(1)_s$. Consequently, magnons are described by a three-component unit-vector field $\vec{e}(x) \in S^2$ in the coset space $S^2 = SU(2)_s/U(1)_s$. Here $x = (x_1, x_2, t)$ is a point in $(2+1)$-dimensional Euclidean space-time and $\vec{e}(x)$ represents the direction of the local staggered magnetization vector: the order parameter for the spontaneously broken spin symmetry. To leading order in a systematic derivative expansion, the Euclidean low-energy effective action for the magnons is given by

$$S[\vec{e}] = \int d^2x\, dt\, \frac{\rho_s}{2}\left(\partial_i\vec{e}\cdot\partial_i\vec{e} + \frac{1}{c^2}\partial_t\vec{e}\cdot\partial_t\vec{e}\right). \qquad (2.1)$$

Here, ρ_s is the spin stiffness and c is the spin-wave velocity. The vacuum configuration of the effective theory is described by a constant staggered magnetization vector which can be chosen to point in the three-direction, i.e., $\vec{e}(x) = (0,0,1)$. Magnons are small fluctuations around the vacuum configuration. It should be noted that, in contrast to a ferromagnet, antiferromagnetic magnons have a "relativistic" dispersion relation.

The most important symmetry of the action is the spontaneously broken spin symmetry $SU(2)_s$. In the following, global transformations in the unbroken subgroup $U(1)_s$ will play an important role. Introducing

$$\vec{e}(x) = (\sin\theta(x)\cos\varphi(x), \sin\theta(x)\sin\varphi(x), \cos\theta(x)), \quad (2.2)$$

these transformations take the form

$$^{I(\gamma)}\vec{e}(x) = (\sin\theta(x)\cos[\varphi(x)+\gamma], \sin\theta(x)\sin[\varphi(x)+\gamma], \cos\theta(x)). \quad (2.3)$$

It should be pointed out that the $SU(2)_s$ spin symmetry plays the role of an internal symmetry (analogous to chiral symmetry in particle physics). Consequently, its unbroken $U(1)_s$ subgroup (which is analogous to isospin in particle physics) should also be viewed as an internal symmetry. Because of the analogy with isospin, we denote transformations in the unbroken subgroup $U(1)_s$ by $I(\gamma)$.

In addition to the $SU(2)_s$ spin symmetry, the effective action has other symmetries as well. First of all, due to the relativistic dispersion relation of antiferromagnetic magnons, the leading terms in the effective action have an emergent accidental Poincaré symmetry which is not present in the underlying Hubbard or t-J model, and which will thus be explicitly broken by higher-order terms in the effective action containing a larger number of derivatives. The remaining symmetries are the discrete translations and rotations of the underlying quadratic lattice. Similar to the spin symmetry, the displacements D_i by one lattice spacing in the i-direction are also spontaneously broken in an antiferromagnet. They act on the staggered magnetization field as

$$^{D_i}\vec{e}(x) = -\vec{e}(x). \tag{2.4}$$

Since the shift symmetries D_i are spontaneously broken in an antiferromagnet, it is convenient to also introduce modified shift symmetries D_i' which combine D_i with an $SU(2)_s$ spin rotation $g = i\sigma_2$ such that

$$^{D_i'}\vec{e}(x) = (e_1(x), -e_2(x), e_3(x)). \tag{2.5}$$

Spatial translations by an even number of lattice spacings, on the other hand, remain unbroken. Such translations $D(x_0)$ by a distance vector $x_0 = (x_{01}, x_{02}, 0)$ act as

$$^{D(x_0)}\vec{e}(x) = \vec{e}(x - x_0). \tag{2.6}$$

Similarly, parametrizing $x = (r\cos\chi, r\sin\chi, t)$, spatial rotations by an angle β act as

$$\begin{aligned} ^{O(\beta)}\vec{e}(x) &= \vec{e}(O(\beta)x), \\ O(\beta)x &= (r\cos(\chi+\beta), r\sin(\chi+\beta), t), \end{aligned} \tag{2.7}$$

and a spatial reflection at the x_1 axis is represented by

$$^{R}\vec{e}(x) = \vec{e}(Rx), \quad Rx = (x_1, -x_2, t) = (r\cos\chi, -r\sin\chi, t). \tag{2.8}$$

Finally, time reversal, which changes the direction of a spin, acts as

$$\begin{aligned} ^{T}\vec{e}(x) &= -\vec{e}(Tx), \\ Tx &= (x_1, x_2, -t) = (r\cos\chi, r\sin\chi, -t). \end{aligned} \tag{2.9}$$

The effective action of Eq. (2.1) is invariant under all these symmetries.

B. Classical skyrmion solutions

In particle physics, skyrmions arise as topological excitations in the pion effective field theory for the strong interactions,[50] which takes the form of a (3 + 1)-dimensional $SU(2)_L \times SU(2)_R = O(4)$ model. In order to distinguish them from their particle physics analogs, the topological excitations in the (2 + 1)-dimensional $O(3)$ model are sometimes denoted as baby-skyrmions. For simplicity, here we also refer to them just as skyrmions. Skyrmions are topologically nontrivial classical solutions of the magnon effective theory with integer winding number

$$n[\vec{e}] = \frac{1}{8\pi}\int d^2x\, \varepsilon_{ij}\vec{e}\cdot[\partial_i\vec{e}\times\partial_j\vec{e}] \in \Pi_2[S^2] = \mathbb{Z} \tag{2.10}$$

in the second homotopy group of the sphere S^2. Correspondingly, there is a topological current

$$j_\mu(x) = \frac{1}{8\pi}\varepsilon_{\mu\nu\rho}\vec{e}(x)\cdot[\partial_\nu\vec{e}(x)\times\partial_\rho\vec{e}(x)], \tag{2.11}$$

which is conserved, i.e., $\partial_\mu j_\mu(x) = 0$, irrespective of the classical equations of motion. The winding number $n[\vec{e}] = \int d^2x\, j_t(x)$ is just the integrated topological charge density. Under the various symmetries, the topological charge density transforms as

$$\begin{aligned} U(1)_s &: \ ^{I(\gamma)}j_t(x) = j_t(x), \\ D_i &: \ ^{D_i}j_t(x) = -j_t(x), \\ D_i' &: \ ^{D_i'}j_t(x) = -j_t(x), \\ O(\beta) &: \ ^{O(\beta)}j_t(x) = j_t(O(\beta)x), \\ R &: \ ^{R}j_t(x) = -j_t(Rx), \\ T &: \ ^{T}j_t(x) = -j_t(Tx). \end{aligned} \tag{2.12}$$

In particular, the winding number changes sign under the displacements D_i and D_i' as well as under the reflection R and under the time reversal T.

Let us consider static classical solutions for which the energy

$$E[\vec{e}] = \int d^2x\, \frac{\rho_s}{2}\partial_i\vec{e}\cdot\partial_i\vec{e} \tag{2.13}$$

is minimized. We can write

$$\begin{aligned} 0 &\leqslant \int d^2x\, (\partial_i\vec{e} \pm \varepsilon_{ij}\partial_j\vec{e}\times\vec{e})^2 \\ &= \int d^2x\, [2\partial_i\vec{e}\cdot\partial_i\vec{e} \pm 2\varepsilon_{ij}\vec{e}\cdot(\partial_i\vec{e}\times\partial_j\vec{e})] \\ &= \frac{4}{\rho_s}E[\vec{e}] \pm 16\pi n[\vec{e}], \end{aligned} \tag{2.14}$$

which implies the Schwarz inequality

$$E[\vec{e}] \geqslant 4\pi\rho_s|n[\vec{e}]|. \tag{2.15}$$

Skyrmions are minima of the energy in the topological sector with $n[\vec{e}] = 1$, while antiskyrmions have $n[\vec{e}] = -1$. At the classical level, both have a rest energy of $\mathcal{M}c^2 = 4\pi\rho_s$. (Anti)skyrmions satisfy the previous inequality as an equality which is possible only if they satisfy the (anti)self-duality equation

$$\partial_i\vec{e} + \sigma\varepsilon_{ij}\partial_j\vec{e}\times\vec{e} = 0. \tag{2.16}$$

Here, $\sigma = \pm 1$ distinguishes between skyrmions and antiskyrmions. It is worth mentioning that static (anti)skyrmions are mathematically equivalent to (anti)instantons of the two-dimensional $O(3)$ model.[51] Using polar coordinates $(x_1, x_2) = r(\cos\chi, \sin\chi)$, a particular (anti)skyrmion configuration is given by

$$\begin{aligned} &\vec{e}_{\sigma,n,\rho}(r,\chi) \\ &= \left(\frac{2r^n\rho^n}{r^{2n}+\rho^{2n}}\cos(n\chi), \frac{2r^n\rho^n\sigma}{r^{2n}+\rho^{2n}}\sin(n\chi), \frac{r^{2n}-\rho^{2n}}{r^{2n}+\rho^{2n}}\right). \end{aligned} \tag{2.17}$$

Depending on the sign of σ, this configuration describes a skyrmion or antiskyrmion of winding number $n[\vec{e}] = \sigma n$ (with $n \in \mathbb{N}_{>0}$) and size ρ centered at the origin. It should be noted that there are many other multiskyrmion configurations with different skyrmions located in different positions. Such configurations would be important in investigations of a skyrmion gas or liquid. Here, we concentrate on a skyrmion centered at a single point, possibly with a larger winding number than just $n = 1$. The winding is chosen to arise from the angular χ

dependence which influences the rotational symmetry of the skyrmion and not from the radial r dependence, which only influences the finer details of the dynamics.

The skyrmion configurations of Eq. (2.17) have a number of zero modes. In particular, their energy remains unchanged when they are shifted to an arbitrary position x, when they are spatially rotated by an arbitrary angle β, or when they are $U(1)_s$ spin rotated by an arbitrary angle γ. Interestingly, spatial rotations and $U(1)_s$ spin rotations act on a skyrmion in a similar manner, i.e.,

$$
\begin{aligned}
{}^{O(\beta)}\vec{e}_{\sigma,n,\rho}(r,\chi) &= \left(\frac{2r^n\rho^n}{r^{2n}+\rho^{2n}}\cos[n(\chi+\beta)], \frac{2r^n\rho^n\sigma}{r^{2n}+\rho^{2n}}\sin[n(\chi+\beta)], \frac{r^{2n}-\rho^{2n}}{r^{2n}+\rho^{2n}}\right),\\
{}^{I(\sigma\gamma)}\vec{e}_{\sigma,n,\rho}(r,\chi) &= \left(\frac{2r^n\rho^n}{r^{2n}+\rho^{2n}}\cos(n\chi+\gamma), \frac{2r^n\rho^n\sigma}{r^{2n}+\rho^{2n}}\sin(n\chi+\gamma), \frac{r^{2n}-\rho^{2n}}{r^{2n}+\rho^{2n}}\right),
\end{aligned}
\tag{2.18}
$$

such that

$$
{}^{I(\sigma\gamma)}\vec{e}_{\sigma,n,\rho}(r,\chi) = {}^{O(\gamma/n)}\vec{e}_{\sigma,n,\rho}(r,\chi). \tag{2.19}
$$

Another zero mode is related to dilations. Indeed, the energy of a skyrmion also remains invariant under changes of the scale parameter ρ. A family of skyrmion configurations is obtained by spin rotating the original skyrmion of Eq. (2.17) by an angle $\sigma\gamma$ and then shifting it by a distance vector x such that

$$
\vec{e}_{\sigma,n,\rho,x,\gamma}(r,\chi) = {}^{D(x)}[{}^{I(\sigma\gamma)}\vec{e}_{\sigma,n,\rho}(r,\chi)]. \tag{2.20}
$$

Under the various unbroken symmetry transformations, the configuration of Eq. (2.20) transforms as

$$
\begin{aligned}
U(1)_s:&\quad {}^{I(\sigma\gamma_0)}\vec{e}_{\sigma,n,\rho,x,\gamma}(r,\chi) = \vec{e}_{\sigma,n,\rho,x,\gamma+\gamma_0}(r,\chi),\\
D_i':&\quad {}^{D_i'}\vec{e}_{\sigma,n,\rho,x,\gamma}(r,\chi) = \vec{e}_{-\sigma,n,\rho,x,\gamma}(r,\chi),\\
D:&\quad {}^{D(x_0)}\vec{e}_{\sigma,n,\rho,x,\gamma}(r,\chi) = \vec{e}_{\sigma,n,\rho,x+x_0,\gamma}(r,\chi),\\
O(\beta):&\quad {}^{O(\beta)}\vec{e}_{\sigma,n,\rho,x,\gamma}(r,\chi) = \vec{e}_{\sigma,n,\rho,O(\beta)x,\gamma+n\beta}(r,\chi),\\
R:&\quad {}^{R}\vec{e}_{\sigma,n,\rho,x,\gamma}(r,\chi) = \vec{e}_{-\sigma,n,\rho,Rx,-\gamma}(r,\chi).
\end{aligned}
\tag{2.21}
$$

It should be noted that the continuous rotations, translations, and dilations are accidental symmetries of the effective theory in the continuum, while the exact symmetries of the underlying microscopic system are restricted to 90° rotations, lattice translations, and $SU(2)_s$ spin rotations. Hence, only the symmetry I, but not the continuous translations and dilations, give rise to exact zero modes. Interestingly, since $O(\gamma/n)$ acts on a skyrmion in the same way as $I(\sigma\gamma)$ [see Eq. (2.19)], the rotational zero mode remains exact even from a microscopic point of view. It is only this mode that affects the symmetry analysis of holes localized on a skyrmion that is presented in Sec. IV.

In particle physics, skyrmions play an interesting role in the effective theory for the strong interactions. In particular, skyrmions arise as topological excitations in the pion field.[50] While skyrmions are outside the validity range of the systematic low-energy expansion of chiral perturbation theory, they have been used to model baryons phenomenologically.[52] Remarkably, the $\Pi_3[S^3]$ topological winding number of the skyrmions of the strong interactions has the same symmetry properties as the baryon number, and is indeed identified with it. The identification of skyrmions as baryons can even be established within the framework of chiral perturbation theory by investigating the electromagnetic interactions of pions which are affected by a Goldstone-Wilczek current.[40,41,53,54] Since the underlying QCD theory has a conserved baryon number current, the conservation of the topological Skyrme current is guaranteed beyond the semiclassical regime.

It is natural to ask whether the winding number $n[\vec{e}] \in \Pi_2[S^2]$ of the skyrmions in an antiferromagnet can also be identified with a conserved quantity of an underlying microscopic system, such as the Hubbard model. In particular, in analogy to particle physics, one might suspect that the winding number can be identified with the fermion number of doped holes. However, this is not the case because the winding number and the fermion number have different symmetry properties. In particular, the winding number changes sign under a shift D_i by one lattice spacing, while the fermion number does not. Hence, unlike in particle physics, in an antiferromagnet the conservation of the topological current is not protected by the underlying microscopic dynamics and may thus be limited to the semiclassical regime. Interestingly, when holes get localized on a skyrmion, they endow the skyrmion with their conserved fermion number, which may stabilize the skyrmion beyond the semiclassical regime.

The conservation of the topological current also plays a central role in the scenario of deconfined quantum criticality[39] in which dynamically generated gauge fields and deconfined spinons are conjectured to appear at a new type of quantum phase transition outside the realm of the standard Ginsburg-Landau-Wilson paradigm. In fact, the suppression of skyrmion number violating (so-called monopole) events has been argued to change the universality class of the phase transition in the $(2+1)$-dimensional $O(3)$ model.[38] A better understanding of the role of skyrmions would thus also be useful for addressing the issue of deconfined quantum criticality.

C. Hopf term

A reader who is only interested in the main results of our study may skip this section. The integer winding number $n[\vec{e}]$ is defined at any instant of time and is conserved for topological reasons. Interestingly, there is another topological invariant, the Hopf number $H[\vec{e}]$, which characterizes the topology of the order parameter field $\vec{e}(x)$ as a function of both space and time. The integer-valued Hopf number $H[\vec{e}] \in \Pi_3[S^2] = \mathbb{Z}$

is an element of the third homotopy group of the sphere S^2. In order to construct the Hopf term, it is most convenient to introduce the $\mathbb{C}P(1)$ representation

$$P(x) = \tfrac{1}{2}[\mathbb{1} + \vec{e}(x)\cdot\vec{\sigma}] \quad (2.22)$$

of the staggered magnetization field. Here, $\vec{\sigma}$ are the Pauli matrices and, as a result, $P(x)$ is a Hermitian 2×2 projector matrix that obeys

$$P(x)^\dagger = P(x), \quad P(x)^2 = P(x), \quad \mathrm{Tr}P(x) = 1. \quad (2.23)$$

Under a spin rotation $g \in SU(2)_s$ the matrix $P(x)$ transforms as

$$P(x)' = gP(x)g^\dagger. \quad (2.24)$$

The matrix $P(x)$ can be diagonalized by a unitary transformation $u(x) \in SU(2)$, i.e.,

$$u(x)P(x)u(x)^\dagger = \frac{1}{2}(\mathbb{1}+\sigma_3) = \begin{pmatrix} 1 & 0 \\ 0 & 0 \end{pmatrix}, \quad u_{11}(x) \geqslant 0. \quad (2.25)$$

We demand that $u_{11}(x)$ is real and positive, which fixes a $U(1)_s$ gauge ambiguity and uniquely determines $u(x)$ as

$$\begin{aligned} u(x) &= \frac{1}{\sqrt{2[1+e_3(x)]}}\begin{pmatrix} 1+e_3(x) & e_1(x) - ie_2(x) \\ -e_1(x) - ie_2(x) & 1+e_3(x)\end{pmatrix} \\ &= \begin{pmatrix} \cos\left[\frac{1}{2}\theta(x)\right] & \sin\left[\frac{1}{2}\theta(x)\right]\exp[-i\varphi(x)] \\ -\sin\left[\frac{1}{2}\theta(x)\right]\exp[i\varphi(x)] & \cos\left[\frac{1}{2}\theta(x)\right]\end{pmatrix} \\ &= \cos\left(\frac{1}{2}\theta(x)\right) + i\sin\left(\frac{1}{2}\theta(x)\right)\vec{e}_\varphi(x)\cdot\vec{\sigma}, \end{aligned} \quad (2.26)$$

where the unit vector $\vec{e}_\varphi(x)$ is given by

$$\vec{e}_\varphi(x) = (-\sin\varphi(x), \cos\varphi(x), 0). \quad (2.27)$$

Under a global $SU(2)_s$ transformation g, the diagonalizing field $u(x)$ transforms as

$$u(x)' = h(x)u(x)g^\dagger, \quad u_{11}(x)' \geqslant 0, \quad (2.28)$$

which implicitly defines the nonlinear symmetry transformation

$$\begin{aligned} h(x) &= \exp[i\alpha(x)\sigma_3] \\ &= \begin{pmatrix} \exp[i\alpha(x)] & 0 \\ 0 & \exp[-i\alpha(x)]\end{pmatrix} \in U(1)_s. \end{aligned} \quad (2.29)$$

In this way, the global transformations $g \in SU(2)_s$ of the spontaneously broken non-Abelian spin symmetry "disguise" themselves as local transformations $h(x) \in U(1)_s$ of the unbroken subgroup. The global subgroup transformations $I(\gamma)$ introduced in Eq. (2.3) simply lead to $\alpha(x) = -\gamma/2$.

The diagonalizing matrix $u(x)$ maps space-time onto the group manifold S^3 of $SU(2)_s$. When the $(2+1)$-dimensional space-time is also compactified to S^3, one can relate the Hopf number $H[\vec{e}] \in \Pi_3[S^2] = \mathbb{Z}$ to the topological winding number $W[u] \in \Pi_3[SU(2)_s] = \Pi_3[S^3] = \mathbb{Z}$, i.e.,

$$\begin{aligned} H[\vec{e}] = W[u] &= \frac{1}{24\pi^2}\int dt\, d^2x\, \varepsilon_{\mu\nu\rho} \\ &\times \mathrm{Tr}[(u^\dagger\partial_\mu u)(u^\dagger\partial_\nu u)(u^\dagger\partial_\rho u)]. \end{aligned} \quad (2.30)$$

It should be noted that the evaluation of Eq. (2.30) requires some care. In particular, due to the $U(1)_s$ gauge fixing $u_{11}(x) \geqslant 0$, $u(x)$ covers only an S^2 subspace of the $SU(2)_s$ group manifold S^3. This may seem to imply that the winding number $W[u]$, which counts the number of times the map $u(x)$ covers S^3, should vanish. However, this is not the case because $u(x)$ in Eq. (2.26) is singular at the skyrmion center where $e_3(x) = -1$ [i.e., $\theta(x) = \pi$]. The singularities which lie on a vortex line encircled by $\vec{e}_\varphi(x)$ contribute nontrivially to Eq. (2.30). Alternatively, one may remove the singularities in $u(x)$ by undoing the $U(1)_s$ gauge fixing $u_{11}(x) \geqslant 0$, which implies that $u(x)$ extends to all of S^3. Then, Eq. (2.30) can be evaluated in a straightforward manner. The Hopf term is $SU(2)_s$ invariant because

$$W[u'] = W[hug^\dagger] = W[h] + W[u] - W[g] = W[u]. \quad (2.31)$$

Here, we have used $W[g] = 0$, which follows because g is constant, and $W[h] = 0$, which follows because the Abelian gauge transformations $h(x) \in U(1)_s$ are topologically trivial in three dimensions, i.e., $\Pi_3[U(1)_s] = \Pi_3[S^1] = \{0\}$.

Under the various relevant symmetries, the Hopf number transforms as

$$\begin{aligned} U(1)_s &: \; H[^{I(\gamma)}\vec{e}] = H[\vec{e}], \\ D_i &: \; H[^{D_i}\vec{e}] = H[\vec{e}], \\ D_i' &: \; H[^{D_i'}\vec{e}] = H[\vec{e}], \\ O(\beta) &: \; H[^{O(\beta)}\vec{e}] = H[\vec{e}], \\ R &: \; H[^{R}\vec{e}] = -H[\vec{e}], \\ T &: \; H[^{T}\vec{e}] = -H[\vec{e}]. \end{aligned} \quad (2.32)$$

The Hopf term gives rise to an additional factor $\exp(i\Theta H[\vec{e}])$ in the Euclidean path integral with Θ being the anyon statistics angle. In systems with reflection or time-reversal symmetry, the value of Θ is hence limited to 0 or π. As we will see, in these cases skyrmions are quantized as bosons or fermions, respectively. In systems without reflection and time-reversal symmetry, arbitrary values of Θ are allowed, and then the skyrmions may have any (neither integer nor half-integer) spin. By investigating field configurations in which two skyrmions interchange their positions, one can also show that skyrmions pick up a phase $\exp(i\Theta)$ and thus obey anyon statistics.[55] It should be noted that the Hopf term is expected to be absent in doped cuprates,[31,32,56–58] while it is known to be present, for example, in quantum Hall ferromagnets.[40,61–63] In order to keep the discussion as general as possible, we will include the Hopf term, although in the cuprates one expects $\Theta = 0$.

D. Collective mode quantization of the skyrmion

Let us now consider the collective mode quantization of the skyrmion. The main goal is to understand the quantum numbers of the quantized skyrmion, first of all in an undoped system. It should be pointed out that skyrmions in an undoped antiferromagnet are heavy objects, the pair creation of which is suppressed at low temperatures. When antiferromagnetism is weakened by hole doping, the skyrmion mass is reduced and, in addition, the holes may lower their mass by getting localized on a skyrmion. This favors skyrmion formation in doped antiferromagnets. A central goal of this paper is to understand the quantum numbers of the skyrmion-hole bound states. In this section, we consider the collective mode quantization of a skyrmion in the undoped system.

In order to perform the collective mode quantization, we consider the zero-mode parameters $\rho(t)$, $x(t)$, and $\gamma(t)$ as functions of time. We now evaluate the Euclidean action (including the Hopf term) for a time-dependent skyrmion and (after a somewhat lengthy but straightforward calculation), we obtain

$$S[\vec{e}_{\sigma,n,\rho,x,\gamma}] + i\Theta H[\vec{e}_{\sigma,n,\rho,x,\gamma}] = \int dt \left(\mathcal{M}c^2 + \frac{\mathcal{M}}{2}\dot{x}^2 + \frac{\mathcal{D}(\rho)}{2}\dot{\rho}^2 + \frac{\mathcal{I}(\rho)}{2}\dot{\gamma}^2 + in\frac{\Theta}{2\pi}\dot{\gamma}\right). \tag{2.33}$$

Here, the skyrmion's rest energy is given by

$$\mathcal{M}c^2 = \rho_s \int d^2x \frac{4n^2\rho^{2n}r^{2n-2}}{(r^{2n}+\rho^{2n})^2} = 4\pi\rho_s n, \tag{2.34}$$

which confirms that for self-dual solutions, the Schwarz inequality of Eq. (2.15) is obeyed as an equality. For $n > 1$, the skyrmion's inertia against dilations takes the form

$$\mathcal{D}(\rho) = \frac{\rho_s}{c^2} \int d^2x \frac{4n^2 r^{2n}\rho^{2n-2}}{(r^{2n}+\rho^{2n})^2} = \frac{\pi\mathcal{M}}{n\sin(\pi/n)}. \tag{2.35}$$

For $n = 1$, the integral is logarithmically infrared divergent. In a finite volume or in a system with a finite density of skyrmions, the infrared divergence may be regularized because the volume available to each skyrmion becomes effectively finite. Indeed, such effects are known to arise in the instanton gas of the two-dimensional $O(3)$ model.[59,60] In this paper, we do not attempt to decide whether the same happens in the $(2+1)$-dimensional $O(3)$ model that is relevant here. We just regularize $\mathcal{D}(\rho)$ by an infrared cutoff R which may or may not be infinite such that for $n = 1$,

$$\mathcal{D}(\rho) = \frac{4\pi\rho_s}{c^2}\int_0^R dr \frac{2r^3}{(r^2+\rho^2)^2} = \mathcal{M}\left(\ln\frac{R^2+\rho^2}{\rho^2} - \frac{R^2}{R^2+\rho^2}\right). \tag{2.36}$$

Finally, the moment of inertia of the skyrmion is given by

$$\mathcal{I}(\rho) = \frac{\rho_s}{c^2}\int d^2x \frac{4r^{2n}\rho^{2n}}{(r^{2n}+\rho^{2n})^2} = \frac{\mathcal{D}(\rho)\rho^2}{n^2}, \tag{2.37}$$

which is affected by the same infrared divergence as $\mathcal{D}(\rho)$. Hence, although the skyrmion has a finite mass (and can thus undergo translational motion), in the limit of an infinite infrared cutoff R it has an infinite moment of inertia $\mathcal{I}(\rho)$ and can thus not rotate.

From the Euclidean action of Eq. (2.33), we read off the real-time Lagrange function as

$$L = \frac{\mathcal{M}}{2}\dot{x}^2 + \frac{\mathcal{D}(\rho)}{2}\left(\dot{\rho}^2 + \frac{\rho^2}{n^2}\dot{\gamma}^2\right) - n\frac{\Theta}{2\pi}\dot{\gamma} - \mathcal{M}c^2. \tag{2.38}$$

In the next step, we consider the canonically conjugate momenta

$$p_i = \frac{\partial L}{\partial \dot{x}_i} = \mathcal{M}\dot{x}_i, \quad p_\rho = \frac{\partial L}{\partial\dot{\rho}} = \mathcal{D}(\rho)\dot{\rho}, \quad p_\gamma = \frac{\partial L}{\partial\dot{\gamma}} = \frac{\mathcal{D}(\rho)\rho^2\dot{\gamma}}{n^2} - n\frac{\Theta}{2\pi}. \tag{2.39}$$

It should be noted that, at the classical level, the Θ term is suppressed because relative to p_γ it is of order $\hbar$ (which we have put to 1). The canonically conjugate momenta lead to the classical Hamilton function

$$\mathcal{H} = p_i\dot{x}_i + p_\rho\dot{\rho} + p_\gamma\dot{\gamma} - L = \mathcal{M}c^2 + \frac{p_i^2}{2\mathcal{M}} + \frac{1}{2\mathcal{D}(\rho)}\left[p_\rho^2 + \frac{n^2}{\rho^2}\left(p_\gamma + n\frac{\Theta}{2\pi}\right)^2\right]. \tag{2.40}$$

The momentum p_i, the spin p_γ, and the energy

$$E = \frac{1}{2\mathcal{D}(\rho)}\left[p_\rho^2 + \frac{n^2}{\rho^2}\left(p_\gamma + n\frac{\Theta}{2\pi}\right)^2\right] = \frac{\mathcal{D}(\rho)}{2}\dot{\rho}^2 + \frac{n^2}{2\mathcal{D}(\rho)\rho^2}\left(p_\gamma + n\frac{\Theta}{2\pi}\right)^2 \tag{2.41}$$

of the coupled rotational and dilational motion are conserved quantities. The last equality determines the size $\rho(t)$ of the skyrmion as a function of time:

$$t = \int_{\rho(0)}^{\rho(t)} d\rho \left[\frac{2E}{\mathcal{D}(\rho)} - \frac{n^2}{\mathcal{D}(\rho)^2\rho^2}\left(p_\gamma + n\frac{\Theta}{2\pi}\right)^2\right]^{-1/2}. \tag{2.42}$$

When the skyrmion is rotating (i.e., when $p_\gamma + n\frac{\Theta}{2\pi} \neq 0$), centrifugal forces lead to an unlimited increase of $\rho(t)$.

Upon canonical quantization, the momentum p_i and the spin p_γ turn into the operators

$$p_i = -i\partial_{x_i}, \quad p_\gamma = -i\partial_\gamma, \tag{2.43}$$

while the classical Hamilton function $\mathcal{H}$ turns into the quantum mechanical Hamiltonian

$$H = \mathcal{M}c^2 - \frac{1}{2\mathcal{M}}\partial_{x_i}^2 - \frac{1}{\sqrt{2\mathcal{D}(\rho)}}\left(\partial_\rho^2 + \frac{1}{\rho}\partial_\rho\right)\frac{1}{\sqrt{2\mathcal{D}(\rho)}} - \frac{n^2}{2\mathcal{D}(\rho)\rho^2}\left(\partial_\gamma + in\frac{\Theta}{2\pi}\right)^2. \tag{2.44}$$

The collective mode wave function of a skyrmion or anti-skyrmion with winding number σn, momentum p_i, and spin $p_\gamma = \sigma m \in \mathbb{Z}$ takes the form

$$\Psi_{p,\sigma,n,m}(x,\rho,\gamma) = \exp(ip_ix_i)\exp(i\sigma m\gamma)\psi(\rho). \tag{2.45}$$

The dilational part of the wave function solves the Schrödinger equation

$$\left[-\frac{1}{\sqrt{2\mathcal{D}(\rho)}}\left(\partial_\rho^2 + \frac{1}{\rho}\partial_\rho\right)\frac{1}{\sqrt{2\mathcal{D}(\rho)}} + \frac{n^2}{2\mathcal{D}(\rho)\rho^2}\left(m + n\sigma\frac{\Theta}{2\pi}\right)^2\right]\psi(\rho) = E\psi(\rho), \tag{2.46}$$

which may again lead to an instability of a rotating skyrmion against unlimited increase of its size ρ. As we will see later, localized holes prevent the increase of ρ and thus stabilize the skyrmion.

In the presence of the Hopf term, the spin operator of the skyrmion (which is analogous to isospin in particle physics) is given by

$$I = \sigma\left(p_\gamma + n\frac{\Theta}{2\pi}\right) = \sigma\left(-i\partial_\gamma + n\frac{\Theta}{2\pi}\right). \quad (2.47)$$

The state $\Psi_{p,\sigma,n,m}(x,\rho,\gamma)$ hence has the "isospin"

$$I\Psi_{p,\sigma,n,m}(x,\rho,\gamma) = \left(m + \sigma n\frac{\Theta}{2\pi}\right)\Psi_{p,\sigma,n,m}(x,\rho,\gamma). \quad (2.48)$$

In particular, for $\Theta = 0$ the "isospin" is an integer, while for $\Theta = \pi$ it is a half-integer for odd n.

Let us also investigate the quantum numbers of the skyrmion with respect to spatial rotations. As a consequence of Eq. (2.19), the angular momentum J is given by

$$J = \sigma n I = n\left(p_\gamma + n\frac{\Theta}{2\pi}\right) = n\left(-i\partial_\gamma + n\frac{\Theta}{2\pi}\right), \quad (2.49)$$

such that

$$J\Psi_{p,\sigma,n,m}(x,\rho,\gamma) = n\left(\sigma m + n\frac{\Theta}{2\pi}\right)\Psi_{p,\sigma,n,m}(x,\rho,\gamma). \quad (2.50)$$

Hence, for $\Theta = 0$ the skyrmion has integer angular momentum and thus is a boson, while for $\Theta = \pi$ the angular momentum is a half-integer for odd n and the skyrmion is a fermion. Interestingly, in $(2+1)$ dimensions, it is possible to have particles of any (neither integer nor half-integer) angular momentum: the anyons which arise for $\Theta \neq 0$ or π.

By construction, the skyrmion state is also an eigenstate of the momentum operator with eigenvalue p_i. Under the modified shift symmetries D_i' and under the reflection R, the skyrmion state transforms as

$$\begin{aligned} U_{D_i'}\Psi_{p,\sigma,n,m}(x,\rho,\gamma) &= \Psi_{p,-\sigma,n,m}(x,\rho,\gamma), \\ U_R\Psi_{p,\sigma,n,m}(x,\rho,\gamma) &= \Psi_{Rp,-\sigma,n,m}(x,\rho,\gamma), \end{aligned} \quad (2.51)$$

where $Rp = (p_1, -p_2)$ is the spatially reflected momentum. Here, $U_{D_i'}$ and U_R are unitary transformations representing the corresponding discrete symmetries in the Hilbert space of the collective modes of the skyrmion. It should be noted that shifted or reflected skyrmions (which have $\sigma = 1$) are actually antiskyrmions (with $\sigma = -1$).

III. EFFECTIVE ACTION FOR DOPED HOLES

In order to make this paper self-contained, in this section we review the main features of the effective field theory constructed in Ref. 14 which couples doped holes to the staggered magnetization order parameter. A reader who is only interested in the main results of our study can skip Sec. III and proceed directly to Sec. IV.

A. Nonlinear realization of the SU(2)$_s$ symmetry

In order to couple holes to the staggered magnetization order parameter, a nonlinear realization of the spontaneously broken SU(2)$_s$ symmetry has been constructed in Ref. 13. The global SU(2)$_s$ symmetry then manifests itself as a local U(1)$_s$ symmetry in the unbroken subgroup. This is analogous to baryon chiral perturbation theory in which the spontaneously broken SU(2)$_L \times$ SU(2)$_R$ chiral symmetry of QCD is implemented on the nucleon fields as a local SU(2)$_{L=R}$ transformation in the unbroken isospin subgroup.

The definition of the nonlinear realization of the SU(2)$_s$ symmetry is based on the diagonalizing matrix $u(x)$ defined in Eq. (2.26), which transforms as

$$^{D_i'}u(x) = u(x)^*, \quad (3.1)$$

under the modified displacement symmetry D_i'. Introducing the traceless anti-Hermitian field

$$v_\mu(x) = u(x)\partial_\mu u(x)^\dagger, \quad (3.2)$$

one obtains the following transformation rules:

$$\begin{aligned} \mathrm{SU}(2)_s:\ & v_\mu(x)' = h(x)[v_\mu(x) + \partial_\mu]h(x)^\dagger, \\ D_i':\ & {}^{D_i'}v_\mu(x) = v_\mu(x)^*, \\ O:\ & {}^{O}v_i(x) = \varepsilon_{ij}v_j(Ox), \quad {}^{O}v_t(x) = v_t(Ox), \\ R:\ & {}^{R}v_1(x) = v_1(Rx), \quad {}^{R}v_2(x) = -v_2(Rx), \\ & {}^{R}v_t(x) = v_t(Rx). \end{aligned} \quad (3.3)$$

Writing

$$v_\mu(x) = iv_\mu^a(x)\sigma_a, \quad v_\mu^\pm(x) = v_\mu^1(x) \mp iv_\mu^2(x), \quad (3.4)$$

the field $v_\mu(x)$ decomposes into an Abelian "gauge" field $v_\mu^3(x)$ and two "charged" vector fields $v_\mu^\pm(x)$.

Using Eq. (2.20), for a skyrmion $\vec{e}_{\sigma,n,\rho,0,\gamma}(r,\chi)$ centered at $x = 0$ one obtains

$$\begin{aligned} v_1^3(r,\chi) &= -\frac{\sigma n\rho^{2n}}{r(r^{2n}+\rho^{2n})}\sin\chi, \\ v_2^3(r,\chi) &= \frac{\sigma n\rho^{2n}}{r(r^{2n}+\rho^{2n})}\cos\chi, \\ v_t^3(r,\chi) &= \frac{\sigma\rho^{2n}}{r^{2n}+\rho^{2n}}\dot{\gamma}, \\ v_1^\pm(r,\chi) &= \mp i\frac{nr^{n-1}\rho^n}{r^{2n}+\rho^{2n}}\exp\{\mp i\sigma\,[(n+1)\chi+\gamma]\}, \\ v_2^\pm(r,\chi) &= \frac{\sigma nr^{n-1}\rho^n}{r^{2n}+\rho^{2n}}\exp\{\mp i\sigma\,[(n+1)\chi+\gamma]\}, \\ v_t^\pm(r,\chi) &= \frac{\sigma r^n\rho^n}{r^{2n}+\rho^{2n}}\exp[\mp i\sigma(n\chi+\gamma)]\dot{\gamma}. \end{aligned} \quad (3.5)$$

In principle, when holes get localized on a skyrmion, they affect the radial profile of the skyrmion. Here, we neglect this effect and concentrate on symmetry considerations which are independent of such details of the dynamics.

B. Hole fields and their transformation properties

As discussed in detail in Ref. 14, the holes are described by Grassmann-valued fields $\psi_\pm^f(x)$. Here, $f \in \{\alpha,\beta\}$ is a flavor index which specifies the momentum space pocket in which the hole resides, and the subscript $\pm$ denotes the spin of the hole relative to the direction of the local staggered magnetization. Under the various relevant symmetries of the underlying antiferromagnet on a square lattice, the hole fields transform as

$$\begin{aligned} SU(2)_s &: \ \psi^f_\pm(x)' = \exp[\pm i\alpha(x)]\psi^f_\pm(x), \\ U(1)_Q &: \ {}^Q\psi^f_\pm(x) = \exp(i\omega)\psi^f_\pm(x), \\ D'_i &: \ {}^{D'_i}\psi^f_\pm(x) = \pm\exp\left(ik^f_i a\right)\psi^f_\mp(x), \\ O &: \ {}^O\psi^\alpha_\pm(x) = \mp\psi^\beta_\pm(Ox), \quad {}^O\psi^\beta_\pm(x) = \psi^\alpha_\pm(Ox), \\ R &: \ {}^R\psi^\alpha_\pm(x) = \psi^\beta_\pm(Rx), \quad {}^R\psi^\beta_\pm(x) = \psi^\alpha_\pm(Rx). \end{aligned} \tag{3.6}$$

The $U(1)_Q$ symmetry is just fermion number, while $k^\alpha = (\frac{\pi}{2a},\frac{\pi}{2a})$ and $k^\beta = (\frac{\pi}{2a},-\frac{\pi}{2a})$ (with a being the lattice spacing) point to the centers of the two hole pockets illustrated in Fig. 1. It is interesting that in the effective theory, momentum indices of the underlying microscopic dynamics turn into internal flavor quantum numbers.

C. Effective action for holes coupled to the staggered magnetization

Based on the above symmetry properties, the leading and subleading terms of the effective action for an antiferromagnet on a square lattice have been constructed systematically in Ref. 14. Here, we restrict ourselves to the leading terms. We also make the simplifying (but somewhat unrealistic) assumption that the momentum-space hole pockets have a circular shape, which enables us to perform large parts of the following calculations analytically. It would be straightforward to take into account the more realistic elliptic shape of the hole pockets, but this would require some numerical work. Here, we concentrate foremost on the symmetry properties of holes localized on a skyrmion on which the simplifying assumption of spherical hole pockets has no effect. The total action of the coupled system including doped holes then takes the form

$$\begin{aligned} S[\psi^{f\dagger}_\pm,\psi^f_\pm,\vec{e}] = \int d^2x\, dt \Bigg\{ \frac{\rho_s}{2}\left(\partial_i\vec{e}\cdot\partial_i\vec{e} + \frac{1}{c^2}\partial_t\vec{e}\cdot\partial_t\vec{e}\right) \\ + \sum_{\substack{f=\alpha,\beta \\ s=+,-}} \left[M\psi^{f\dagger}_s\psi^f_s + \psi^{f\dagger}_s D_t\psi^f_s + \frac{1}{2M'}D_i\psi^{f\dagger}_s D_i\psi^f_s + \Lambda\left(\psi^{f\dagger}_s v^s_1\psi^f_{-s} + \sigma_f\psi^{f\dagger}_s v^s_2\psi^f_{-s}\right)\right]\Bigg\}. \end{aligned} \tag{3.7}$$

Here, M and M' are the rest energy and the kinetic mass of a hole, and Λ is the hole-one-magnon coupling constant. The sign σ_f is $+$ for $f=\alpha$ and $-$ for $f=\beta$. The covariant derivatives are given by

$$D_\mu\psi^f_\pm(x) = \left[\partial_\mu \pm i v^3_\mu(x)\right]\psi^f_\pm(x). \tag{3.8}$$

Remarkably, the Shraiman-Siggia term in the action, which is proportional to Λ, contains just a single (uncontracted) spatial derivative. Due to the nontrivial rotation properties of flavor, this term is still 90° rotation invariant. Due to the small number of derivatives it contains, this term dominates the low-energy dynamics. In particular, it alone is responsible for one-magnon exchange between hole pairs[14,24] as well as for potential spiral phases in the staggered magnetization order parameter.[25] It is interesting to note that a similar term is absent in lightly electron-doped antiferromagnets,[30] such that spiral phases do not arise in these systems.

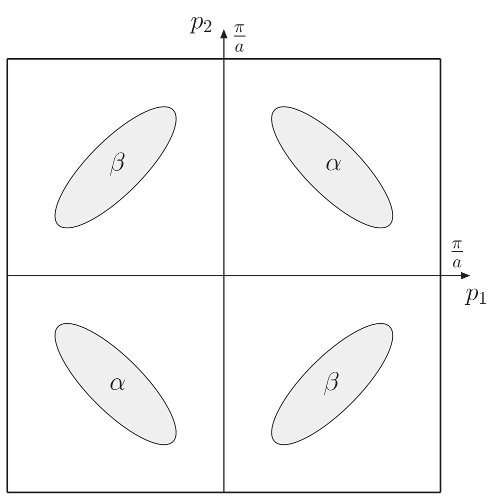

FIG. 1. Elliptically shaped hole pockets centered at $(\pm\frac{\pi}{2a},\pm\frac{\pi}{2a})$. Two half-pockets combine to form the pockets for the flavors $f=\alpha,\beta$.

IV. HOLE LOCALIZATION ON A SKYRMION

In this section, we apply the effective theory of the previous section to the localization of holes on a skyrmion. First, we consider the localization of a single hole first on a static and then on a rotating skyrmion. Then, the localization of two holes on the same skyrmion is considered, and the symmetry properties of the resulting two-hole bound states are analyzed.

A. Single hole localized on a static skyrmion

As we have seen, the moment of inertia $\mathcal{I}(\rho)$ of a skyrmion with $n=1$ is logarithmically divergent in the infrared. Unless the divergence is regularized due to a finite spatial volume or the presence of other skyrmions, the skyrmion then can not rotate. In the interest of analytic solubility, and because we want to focus on symmetry aspects, we will no longer consider the translational and dilational motion of the skyrmion. Instead, we fix the skyrmion center at the origin $x=0$ and we fix the skyrmion size to a constant ρ. As we will see later, in the presence of holes, the energy of the skyrmion-hole bound states is minimized for a particular value of ρ.

The wave function of a single hole localized on a skyrmion takes the form

$$\Psi^f_{\sigma,n}(r,\chi) = \begin{pmatrix} \Psi^f_{\sigma,n,+}(r,\chi) \\ \Psi^f_{\sigma,n,-}(r,\chi) \end{pmatrix}. \tag{4.1}$$

Omitting the constant rest energy M of the holes, which just amounts to a constant energy shift, the corresponding Hamiltonian resulting from the action of Eq. (3.7) is given by

$$\begin{aligned} H^f &= \begin{pmatrix} H^f_{++} & H^f_{+-} \\ H^f_{-+} & H^f_{--} \end{pmatrix}, \\ H^f_{++} &= -\frac{1}{2M'}\left[\partial_i + i v^3_i(x)\right]^2 = -\frac{1}{2M'}\left[\partial_r^2 + \frac{1}{r}\partial_r + \frac{1}{r^2}\left(\partial_\chi + i\frac{\sigma n \rho^{2n}}{r^{2n}+\rho^{2n}}\right)^2\right], \\ H^f_{+-} &= \Lambda[v^+_1(x) + \sigma_f v^+_2(x)] = \sqrt{2}\Lambda\sigma\sigma_f\frac{n r^{n-1}\rho^n}{r^{2n}+\rho^{2n}}\exp\left\{-i\sigma\left[(n+1)\chi + \gamma + \sigma_f\frac{\pi}{4}\right]\right\}, \\ H^f_{-+} &= \Lambda[v^-_1(x) + \sigma_f v^-_2(x)] = \sqrt{2}\Lambda\sigma\sigma_f\frac{n r^{n-1}\rho^n}{r^{2n}+\rho^{2n}}\exp\left\{i\sigma\left[(n+1)\chi + \gamma + \sigma_f\frac{\pi}{4}\right]\right\}, \\ H^f_{--} &= -\frac{1}{2M'}\left[\partial_i - i v^3_i(x)\right]^2 = -\frac{1}{2M'}\left[\partial_r^2 + \frac{1}{r}\partial_r + \frac{1}{r^2}\left(\partial_\chi - i\frac{\sigma n \rho^{2n}}{r^{2n}+\rho^{2n}}\right)^2\right]. \end{aligned} \tag{4.2}$$

Using the explicit form of $v^3_i(x)$ and $v^\pm_i(x)$ for the skyrmion of Eq. (3.5) and making the ansatz

$$\Psi^f_{\sigma,m_+,m_-}(r,\chi) = \begin{pmatrix} \psi_{m_+,m_-,+}(r)\exp\left(i\sigma\left[m_+\chi - \frac{\gamma}{2} - \sigma_f\frac{\pi}{8}\right]\right) \\ \sigma\sigma_f\psi_{m_+,m_-,-}(r)\exp\left(i\sigma\left[m_-\chi + \frac{\gamma}{2} + \sigma_f\frac{\pi}{8}\right]\right) \end{pmatrix}, \tag{4.3}$$

with $m_- - m_+ = n + 1$, after some algebra one obtains the radial Schrödinger equation

$$H_r\psi_{m_+,m_-}(r) = \begin{pmatrix} H_{r++} & H_{r+-} \\ H_{r-+} & H_{r--} \end{pmatrix}\begin{pmatrix} \psi_{m_+,m_-,+}(r) \\ \psi_{m_+,m_-,-}(r) \end{pmatrix} = E_{m_+,m_-}\psi_{m_+,m_-}(r), \tag{4.4}$$

with

$$\begin{aligned} H_{r++} &= -\frac{1}{2M'}\left[\partial_r^2 + \frac{1}{r}\partial_r - \frac{1}{r^2}\left(m_+ + \frac{n\rho^{2n}}{r^{2n}+\rho^{2n}}\right)^2\right], \\ H_{r+-} &= H_{r-+} = \sqrt{2}\Lambda\frac{n r^{n-1}\rho^n}{r^{2n}+\rho^{2n}}, \\ H_{r--} &= -\frac{1}{2M'}\left[\partial_r^2 + \frac{1}{r}\partial_r - \frac{1}{r^2}\left(m_- - \frac{n\rho^{2n}}{r^{2n}+\rho^{2n}}\right)^2\right]. \end{aligned} \tag{4.5}$$

It should be noted that the resulting radial Schrödinger equation is the same for skyrmions and antiskyrmions as well as for both flavors $f = \alpha,\beta$. Interestingly, for odd n and $m_- = -m_+ = (n+1)/2$, the two equations decouple. The equation that leads to a localized hole takes the form

$$\left\{-\frac{1}{2M'}\left[\partial_r^2 + \frac{1}{r}\partial_r - \frac{1}{r^2}\left(\frac{n+1}{2} - \frac{n\rho^{2n}}{r^{2n}+\rho^{2n}}\right)^2\right] - \frac{\sqrt{2}\Lambda n r^{n-1}\rho^n}{r^{2n}+\rho^{2n}}\right\}\psi(r) = E\psi(r), \tag{4.6}$$

where $\psi(r)$ is the linear combination

$$\psi(r) = \frac{1}{\sqrt{2}}[\psi_{m_+,m_-,+}(r) - \psi_{m_+,m_-,-}(r)]. \tag{4.7}$$

For even winding number n, on the other hand, the two equations do not decouple. In the following, we will be most interested in skyrmions (or antiskyrmions) with winding number $n = 1$.

In this paper, we concentrate on the symmetry properties of holes localized on a skyrmion, not paying much attention to finer details of the dynamics. Hence, here we do not solve the radial equation, which would be straightforward using numerical methods. Still, we want to obtain at least a rough estimate for the ground-state energy of a hole localized on a skyrmion. For $n = 1$, the radial Schrödinger equation takes the form

$$\left[-\frac{1}{2M'}\left(\partial_r^2 + \frac{1}{r}\partial_r\right) + V(r)\right]\psi(r) = E\psi(r), \tag{4.8}$$

with the potential given by

$$V(r) = \frac{1}{2M'}\frac{r^2}{(r^2+\rho^2)^2} - \sqrt{2}\Lambda\frac{\rho}{r^2+\rho^2}. \tag{4.9}$$

At short distances, the potential can be approximated by a harmonic oscillator

$$V_{\text{approx}}(r) = -\frac{\sqrt{2}\Lambda}{\rho} + \frac{M'}{2}\left(\frac{1}{M'^2\rho^4} + \frac{2\sqrt{2}\Lambda}{M'\rho^3}\right)r^2 + \mathcal{O}(r^4), \tag{4.10}$$

and hence, in a rather crude harmonic approximation, the ground-state energy takes the form

$$E_0 = -\frac{\sqrt{2}\Lambda}{\rho} + \sqrt{\frac{1}{M'^2\rho^4} + \frac{2\sqrt{2}\Lambda}{M'\rho^3}} = M'\Lambda^2 x\left(\sqrt{x^2+2\sqrt{2}x} - \sqrt{2}\right), \quad x = \frac{1}{M'\Lambda\rho}. \tag{4.11}$$

Minimizing the energy as a function of x yields $x^3 + 3\sqrt{2}x^2 + 4x = \sqrt{2}$, which is solved by

$$x = \sqrt{\frac{2}{3}}\left[\left(\frac{3\sqrt{3}}{4} + \frac{\sqrt{11}}{4}\right)^{1/3} + \left(\frac{3\sqrt{3}}{4} + \frac{\sqrt{11}}{4}\right)^{-1/3}\right] - \sqrt{2} \approx 0.271 \Rightarrow \rho \approx \frac{1}{0.271M'\Lambda}. \tag{4.12}$$

This shows that the presence of the hole explicitly breaks the scale invariance that led to the dilational instability of the pure skyrmion. The resulting bound state with the strongest binding energy has

$$E_0 = M'\Lambda^2 x\left(\sqrt{x^2+2\sqrt{2}x} - \sqrt{2}\right) \approx -0.135M'\Lambda^2. \tag{4.13}$$

The potential $V(r)$ is shown in Fig. 2 together with its harmonic approximation and the corresponding ground-state energy E_0. The figure implies that the true ground-state energy is smaller than the harmonic approximation suggests.

B. Single hole localized on a rotating skyrmion

In this section, we consider a single hole localized on a rotating skyrmion. When the moment of inertia $\mathcal{I}(\rho)$ diverges (as it is the case for $n=1$ and $R=\infty$) the fixed orientation γ of the skyrmion explicitly breaks the $U(1)_s$ symmetry and the analysis of Sec. IV A applies. Here, we assume that $\mathcal{I}(\rho) = \mathcal{D}(\rho)\rho^2/n^2$ is finite. When $\mathcal{I}(\rho)$ is finite, the skyrmion can rotate and thus γ becomes a dynamical variable.

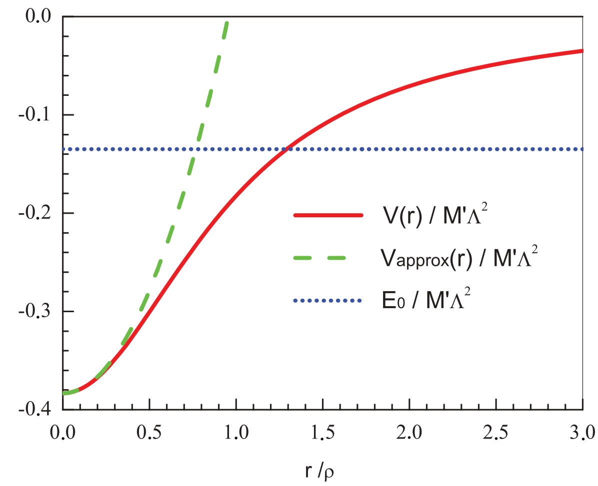

FIG. 2. (Color online) The potential $V(r)$ (solid curve) together with its harmonic approximation (dashed curve) and the corresponding ground-state energy (dotted line).

The γ-dependent terms in the Lagrange function for the rotational motion are given by

$$L = \frac{\mathcal{D}(\rho)\rho^2}{2n^2}\dot{\gamma}^2 - n\frac{\Theta}{2\pi}\dot{\gamma} + \int d^2x \sum_{\substack{f=\alpha,\beta\\ s=+,-}} s\psi_s^{f\dagger}v_t^3\psi_s^f. \tag{4.14}$$

Using Eq. (3.5), the momentum canonically conjugate to γ thus takes the form

$$p_\gamma = \frac{\mathcal{D}(\rho)\rho^2\dot{\gamma}}{n^2} - n\frac{\Theta}{2\pi} + \int d^2x\, \sigma\frac{\rho^{2n}}{r^{2n}+\rho^{2n}} \sum_{\substack{f=\alpha,\beta\\ s=+,-}} s\psi_s^{f\dagger}\psi_s^f, \tag{4.15}$$

which leads to the corresponding Hamiltonian

$$H^\gamma = \frac{1}{2\mathcal{I}(\rho)}(-i\partial_\gamma - A_\gamma)^2, \tag{4.16}$$

with the Berry gauge field

$$A_\gamma = \int d^2x \sum_{\substack{f=\alpha,\beta\\ s=+,-}} \Psi_s^{f\dagger}\frac{\sigma\rho^{2n}}{r^{2n}+\rho^{2n}}s\Psi_s^f - n\frac{\Theta}{2\pi}. \tag{4.17}$$

By combining the results, one sees that while the off-diagonal elements of the Hamiltonian (4.2) remain the same, the diagonal elements receive additional contributions such that now

$$H_{++}^f = -\frac{1}{2M'}\left[\partial_i + iv_i^3(x)\right]^2 - \frac{n^2}{2\mathcal{D}(\rho)\rho^2}\left(\partial_\gamma + in\frac{\Theta}{2\pi} - i\sigma\frac{\rho^{2n}}{r^{2n}+\rho^{2n}}\right)^2 = -\frac{1}{2M'}\left[\partial_r^2 + \frac{1}{r}\partial_r + \frac{1}{r^2}\left(\partial_\chi + i\sigma\frac{n\rho^{2n}}{r^{2n}+\rho^{2n}}\right)^2\right]$$
$$- \frac{n^2}{2\mathcal{D}(\rho)\rho^2}\left(\partial_\gamma + in\frac{\Theta}{2\pi} - i\sigma\frac{\rho^{2n}}{r^{2n}+\rho^{2n}}\right)^2,$$
$$H_{+-}^f = \Lambda[v_1^+(x) + \sigma_f v_2^+(x)] = \sqrt{2}\Lambda\sigma\sigma_f\frac{nr^{n-1}\rho^n}{r^{2n}+\rho^{2n}}\exp\left\{-i\sigma\left[(n+1)\chi + \gamma + \sigma_f\frac{\pi}{4}\right]\right\},$$

$$H^f_{-+} = \Lambda[v_1^-(x) + \sigma_f v_2^-(x)] = \sqrt{2}\Lambda\sigma\sigma_f \frac{n r^{n-1}\rho^n}{r^{2n}+\rho^{2n}} \exp\left\{i\sigma\left[(n+1)\chi + \gamma + \sigma_f\frac{\pi}{4}\right]\right\},$$

$$H^f_{--} = -\frac{1}{2M'}\left[\partial_i - i v_i^3(x)\right]^2 - \frac{n^2}{2\mathcal{D}(\rho)\rho^2}\left(\partial_\gamma + in\frac{\Theta}{2\pi} + i\sigma\frac{\rho^{2n}}{r^{2n}+\rho^{2n}}\right)^2 = -\frac{1}{2M'}\left[\partial_r^2 + \frac{1}{r}\partial_r + \frac{1}{r^2}\left(\partial_\chi - i\sigma\frac{n\rho^{2n}}{r^{2n}+\rho^{2n}}\right)^2\right]$$
$$- \frac{n^2}{2\mathcal{D}(\rho)\rho^2}\left(\partial_\gamma + in\frac{\Theta}{2\pi} + i\sigma\frac{\rho^{2n}}{r^{2n}+\rho^{2n}}\right)^2. \quad (4.18)$$

We now make the ansatz

$$\Psi^f_{\sigma,m_+,m_-,m}(r,\chi,\gamma) = \begin{pmatrix} \psi_{\sigma,m_+,m_-,m,+}(r)\exp\left(i\sigma\left[m_+\chi - \sigma_f\frac{\pi}{8}\right]\right)\exp\left[i\sigma\left(m-\frac{1}{2}\right)\gamma\right] \\ \sigma\sigma_f\psi_{\sigma,m_+,m_-,m,-}(r)\exp\left(i\sigma\left[m_-\chi + \sigma_f\frac{\pi}{8}\right]\right)\exp\left[i\sigma\left(m+\frac{1}{2}\right)\gamma\right]\end{pmatrix} \quad (4.19)$$

with $m_- - m_+ = n + 1$. In order to ensure 2π periodicity of the wave function in the variable γ, m must now be one-half of some odd integer. This is in contrast to the rotating skyrmion without a hole that was discussed in Sec. II D, for which m was an integer. The radial Schrödinger equation is then given by

$$H_r\psi_{\sigma,m_+,m_-,m}(r) = \begin{pmatrix} H_{r++} & H_{r+-} \\ H_{r-+} & H_{r--}\end{pmatrix}\begin{pmatrix}\psi_{\sigma,m_+,m_-,m,+}(r) \\ \psi_{\sigma,m_+,m_-,m,-}(r)\end{pmatrix} = E_{\sigma,m_+,m_-,m}\psi_{\sigma,m_+,m_-,m}(r). \quad (4.20)$$

In this case, the four matrix elements of the radial Hamiltonian H_r take the form

$$H_{r++} = -\frac{1}{2M'}\left[\partial_r^2 + \frac{1}{r}\partial_r - \frac{1}{r^2}\left(m_+ + \frac{n\rho^{2n}}{r^{2n}+\rho^{2n}}\right)^2\right] + \frac{n^2}{2\mathcal{D}(\rho)\rho^2}\left(m + \sigma n\frac{\Theta}{2\pi} - \frac{1}{2} - \frac{\rho^{2n}}{r^{2n}+\rho^{2n}}\right)^2,$$
$$H_{r+-} = H_{r-+} = \sqrt{2}\Lambda\frac{n r^{n-1}\rho^n}{r^{2n}+\rho^{2n}},$$
$$H_{r--} = -\frac{1}{2M'}\left[\partial_r^2 + \frac{1}{r}\partial_r - \frac{1}{r^2}\left(m_- - \frac{n\rho^{2n}}{r^{2n}+\rho^{2n}}\right)^2\right] + \frac{n^2}{2\mathcal{D}(\rho)\rho^2}\left(m + \sigma n\frac{\Theta}{2\pi} + \frac{1}{2} + \frac{\rho^{2n}}{r^{2n}+\rho^{2n}}\right)^2. \quad (4.21)$$

C. Symmetry properties of a single hole localized on a skyrmion

Let us again consider the spin operator (which generates an internal symmetry and is thus analogous to isospin in particle physics)

$$I = \begin{pmatrix} -i\sigma\partial_\gamma + \sigma n\frac{\Theta}{2\pi} + \frac{1}{2} & 0 \\ 0 & -i\sigma\partial_\gamma + \sigma n\frac{\Theta}{2\pi} - \frac{1}{2}\end{pmatrix}, \quad (4.22)$$

which commutes with the Hamiltonian, i.e., $[H^f, I] = 0$. The wave function $\Psi^f_{\sigma,m_+,m_-,m}$ is indeed an eigenstate of I, i.e.,

$$I\ \Psi^f_{\sigma,m_+,m_-,m}(r,\chi,\gamma) = \left(m + \sigma n\frac{\Theta}{2\pi}\right)\Psi^f_{\sigma,m_+,m_-,m}(r,\chi,\gamma). \quad (4.23)$$

Since m is half of an odd integer, the rotating skyrmion with one hole localized on it has half-integer spin (or "isospin"), at least for vanishing anyon statistics parameter $\Theta = 0$.

The various symmetries such as the displacements D_1' and D_2', the 90° rotation O, as well as the reflection R, act on the wave function

$$\Psi^f_{\sigma,n}(r,\chi,\gamma) = \begin{pmatrix}\Psi^f_{\sigma,n,+}(r,\chi,\gamma) \\ \Psi^f_{\sigma,n,-}(r,\chi,\gamma)\end{pmatrix} \quad (4.24)$$

of a single hole localized on a rotating (anti)skyrmion with winding number σn as follows:

$$^{D_i'}\Psi^f_{\sigma,n}(r,\chi,\gamma) = \exp\left(ik_i^f a\right)\begin{pmatrix}\Psi^f_{\sigma,n,-}(r,\chi,\gamma) \\ -\Psi^f_{\sigma,n,+}(r,\chi,\gamma)\end{pmatrix},$$
$$^{O}\Psi^f_{\sigma,n}(r,\chi,\gamma) = \begin{pmatrix}\sigma_f\Psi^f_{\sigma,n,+}\left(r,\chi+\frac{\pi}{2},\gamma - n\frac{\pi}{2}\right) \\ \Psi^f_{\sigma,n,-}\left(r,\chi+\frac{\pi}{2},\gamma - n\frac{\pi}{2}\right)\end{pmatrix},$$
$$^{R}\Psi^f_{\sigma,n}(r,\chi,\gamma) = \begin{pmatrix}\Psi^f_{\sigma,n,+}(r,-\chi,-\gamma) \\ \Psi^f_{\sigma,n,-}(r,-\chi,-\gamma)\end{pmatrix}. \quad (4.25)$$

For energy eigenstates, this then implies

$$^{D_i'}\Psi^f_{\sigma,m_+,m_-,m}(r,\chi,\gamma) = \sigma\sigma_f\exp\left(ik_i^f a\right)\Psi^f_{-\sigma,-m_-,-m_+,-m}(r,\chi,\gamma),$$
$$^{O}\Psi^\alpha_{\sigma,m_+,m_-,m}(r,\chi,\gamma) = \exp\left(i\sigma[m_+ + m_- - 2 - 2nm]\frac{\pi}{4}\right)\Psi^\beta_{\sigma,m_+,m_-,m}(r,\chi,\gamma),$$
$$^{O}\Psi^\beta_{\sigma,m_+,m_-,m}(r,\chi,\gamma) = -\exp\left(i\sigma[m_+ + m_- - 2nm]\frac{\pi}{4}\right)\Psi^\alpha_{\sigma,m_+,m_-,m}(r,\chi,\gamma),$$
$$^{R}\Psi^\alpha_{\sigma,m_+,m_-,m}(r,\chi,\gamma) = \Psi^\beta_{-\sigma,m_+,m_-,m}(r,\chi,\gamma),$$
$$^{R}\Psi^\beta_{\sigma,m_+,m_-,m}(r,\chi,\gamma) = \Psi^\alpha_{-\sigma,m_+,m_-,m}(r,\chi,\gamma). \quad (4.26)$$

It should be noted that for $\Theta \neq 0$ or π, the reflection symmetry R is explicitly broken by the Hopf term. Assuming appropriate phase conventions for the radial wave functions, in the considerations of the shift symmetries D_i', we have used

$$\psi_{-m_-,-m_+,-m,+}(r) = \psi_{m_+,m_-,m,-}(r),$$
$$\psi_{-m_-,-m_+,-m,-}(r) = \psi_{m_+,m_-,m,+}(r), \quad (4.27)$$

which follows from the behavior of Eq. (4.21) under the replacement of $m_+ \to m'_+ = -m_-$, $m_- \to m'_- = -m_+$, and $m \to m' = -m$. It is worth noting that after this replacement, the constraint

$$m'_- - m'_+ = -m_+ + m_- = n + 1 \tag{4.28}$$

remains satisfied.

D. Schrödinger equation for a pair of holes of different flavor localized on a rotating skyrmion

Let us now consider bound states of two holes localized on the same skyrmion. Both a hole of flavor α and another hole of flavor β can occupy the same single-particle ground state in a skyrmion. For holes of the same flavor, this would be forbidden by the Pauli principle. Since we are most interested in the lowest-energy states, we consider two holes of different flavor. The case of two holes with the same flavor is discussed in the Appendix. The Hamiltonian for two holes of different flavor α and β is given by

$$H = H^\alpha + H^\beta + H^\gamma, \tag{4.29}$$

where H^α and H^β are the Hamiltonians for a hole of flavor α and β, respectively. Explicitly, one has

$$H^\alpha = \begin{pmatrix} H^\alpha_{++} & 0 & H^\alpha_{+-} & 0 \\ 0 & H^\alpha_{++} & 0 & H^\alpha_{+-} \\ H^\alpha_{-+} & 0 & H^\alpha_{--} & 0 \\ 0 & H^\alpha_{-+} & 0 & H^\alpha_{--} \end{pmatrix}, \quad H^\beta = \begin{pmatrix} H^\beta_{++} & H^\beta_{+-} & 0 & 0 \\ H^\beta_{-+} & H^\beta_{--} & 0 & 0 \\ 0 & 0 & H^\beta_{++} & H^\beta_{+-} \\ 0 & 0 & H^\beta_{-+} & H^\beta_{--} \end{pmatrix},$$
$$H^\gamma = \begin{pmatrix} H^\gamma_{++++} & 0 & 0 & 0 \\ 0 & H^\gamma_{+-+-} & 0 & 0 \\ 0 & 0 & H^\gamma_{-+-+} & 0 \\ 0 & 0 & 0 & H^\gamma_{----} \end{pmatrix}, \tag{4.30}$$

with

$$\begin{aligned}
H^\alpha_{++} &= -\frac{1}{2M'}\left[\partial_i + i v^3_i(x)\right]^2, \quad H^\alpha_{+-} = \Lambda[v^+_1(x) + v^+_2(x)],\\
H^\alpha_{--} &= -\frac{1}{2M'}\left[\partial_i - i v^3_i(x)\right]^2, \quad H^\alpha_{-+} = \Lambda[v^-_1(x) + v^-_2(x)],\\
H^\beta_{++} &= -\frac{1}{2M'}\left[\partial_i + i v^3_i(x)\right]^2, \quad H^\beta_{+-} = \Lambda[v^+_1(x) - v^+_2(x)],\\
H^\beta_{--} &= -\frac{1}{2M'}\left[\partial_i - i v^3_i(x)\right]^2, \quad H^\beta_{-+} = \Lambda[v^-_1(x) - v^-_2(x)],\\
H^\gamma_{++++} &= -\frac{n^2}{2\mathcal{D}(\rho)\rho^2}\left(\partial_\gamma + in\frac{\Theta}{2\pi} - i\sigma\frac{\rho^{2n}}{r_\alpha^{2n}+\rho^{2n}} - i\sigma\frac{\rho^{2n}}{r_\beta^{2n}+\rho^{2n}}\right)^2,\\
H^\gamma_{+-+-} &= -\frac{n^2}{2\mathcal{D}(\rho)\rho^2}\left(\partial_\gamma + in\frac{\Theta}{2\pi} - i\sigma\frac{\rho^{2n}}{r_\alpha^{2n}+\rho^{2n}} + i\sigma\frac{\rho^{2n}}{r_\beta^{2n}+\rho^{2n}}\right)^2,\\
H^\gamma_{-+-+} &= -\frac{n^2}{2\mathcal{D}(\rho)\rho^2}\left(\partial_\gamma + in\frac{\Theta}{2\pi} + i\sigma\frac{\rho^{2n}}{r_\alpha^{2n}+\rho^{2n}} - i\sigma\frac{\rho^{2n}}{r_\beta^{2n}+\rho^{2n}}\right)^2,\\
H^\gamma_{----} &= -\frac{n^2}{2\mathcal{D}(\rho)\rho^2}\left(\partial_\gamma + in\frac{\Theta}{2\pi} + i\sigma\frac{\rho^{2n}}{r_\alpha^{2n}+\rho^{2n}} + i\sigma\frac{\rho^{2n}}{r_\beta^{2n}+\rho^{2n}}\right)^2.
\end{aligned} \tag{4.31}$$

We now make the following ansatz for a two-hole energy eigenstate:

$$\begin{aligned}
&\Psi^{\alpha\beta}_{\sigma,m^\alpha_+,m^\alpha_-,m^\beta_+,m^\beta_-,m}(r_\alpha,\chi_\alpha,r_\beta,\chi_\beta,\gamma)\\
&= \begin{pmatrix} \psi_{\sigma,m^\alpha_+,m^\alpha_-,m^\beta_+,m^\beta_-,m,++}(r_\alpha,r_\beta)\exp(i\sigma[m^\alpha_+\chi_\alpha + m^\beta_+\chi_\beta])\exp[i\sigma(m-1)\gamma] \\ -\sigma\psi_{\sigma,m^\alpha_+,m^\alpha_-,m^\beta_+,m^\beta_-,m,+-}(r_\alpha,r_\beta)\exp(i\sigma[m^\alpha_+\chi_\alpha + m^\beta_-\chi_\beta - \frac{\pi}{4}])\exp(i\sigma m\gamma) \\ \sigma\psi_{\sigma,m^\alpha_+,m^\alpha_-,m^\beta_+,m^\beta_-,m,-+}(r_\alpha,r_\beta)\exp(i\sigma[m^\alpha_-\chi_\alpha + m^\beta_+\chi_\beta + \frac{\pi}{4}])\exp(i\sigma m\gamma) \\ -\psi_{\sigma,m^\alpha_+,m^\alpha_-,m^\beta_+,m^\beta_-,m,--}(r_\alpha,r_\beta)\exp(i\sigma[m^\alpha_-\chi_\alpha + m^\beta_-\chi_\beta])\exp[i\sigma(m+1)\gamma] \end{pmatrix}.
\end{aligned} \tag{4.32}$$

Again, this solves the Schrödinger equation only if $m_-^f - m_+^f = n + 1$. As for the skyrmion without holes, in this case, m is again an integer. The resulting radial Schrödinger equation then takes the form

$$H_r \psi_{\sigma,m_+^\alpha,m_-^\alpha,m_+^\beta,m_-^\beta,m}(r_\alpha,r_\beta) = E_{\sigma,m_+^\alpha,m_-^\alpha,m_+^\beta,m_-^\beta,m} \psi_{\sigma,m_+^\alpha,m_-^\alpha,m_+^\beta,m_-^\beta,m}(r_\alpha,r_\beta), \tag{4.33}$$

with

$$\psi_{\sigma,m_+^\alpha,m_-^\alpha,m_+^\beta,m_-^\beta,m}(r_\alpha,r_\beta) = \begin{pmatrix} \psi_{\sigma,m_+^\alpha,m_-^\alpha,m_+^\beta,m_-^\beta,m,++}(r_\alpha,r_\beta) \\ \psi_{\sigma,m_+^\alpha,m_-^\alpha,m_+^\beta,m_-^\beta,m,+-}(r_\alpha,r_\beta) \\ \psi_{\sigma,m_+^\alpha,m_-^\alpha,m_+^\beta,m_-^\beta,m,-+}(r_\alpha,r_\beta) \\ \psi_{\sigma,m_+^\alpha,m_-^\alpha,m_+^\beta,m_-^\beta,m,--}(r_\alpha,r_\beta) \end{pmatrix}. \tag{4.34}$$

The radial Hamiltonian is given by

$$H_r = H_r^\alpha + H_r^\beta + H_r^\gamma, \tag{4.35}$$

with

$$H_r^\alpha = \begin{pmatrix} H_{r++}^\alpha & 0 & H_{r+-}^\alpha & 0 \\ 0 & H_{r++}^\alpha & 0 & H_{r+-}^\alpha \\ H_{r-+}^\alpha & 0 & H_{r--}^\alpha & 0 \\ 0 & H_{r-+}^\alpha & 0 & H_{r--}^\alpha \end{pmatrix}, \quad H_r^\beta = \begin{pmatrix} H_{r++}^\beta & H_{r+-}^\beta & 0 & 0 \\ H_{r-+}^\beta & H_{r--}^\beta & 0 & 0 \\ 0 & 0 & H_{r++}^\beta & H_{r+-}^\beta \\ 0 & 0 & H_{r-+}^\beta & H_{r--}^\beta \end{pmatrix},$$
$$H_r^\gamma = \begin{pmatrix} H_{r++++}^\gamma & 0 & 0 & 0 \\ 0 & H_{r+-+-}^\gamma & 0 & 0 \\ 0 & 0 & H_{r-+-+}^\gamma & 0 \\ 0 & 0 & 0 & H_{r----}^\gamma \end{pmatrix}. \tag{4.36}$$

The matrix elements of the fermionic part of the radial Hamiltonian are

$$\begin{aligned} H_{r++}^f &= -\frac{1}{2M'}\left[\partial_{r_f}^2 + \frac{1}{r_f}\partial_{r_f} - \frac{1}{r_f^2}\left(m_+^f + \frac{n\rho^{2n}}{r_f^{2n}+\rho^{2n}}\right)^2\right], \\ H_{r+-}^f &= H_{r-+}^f = \sqrt{2}\Lambda\frac{n r_f^{n-1}\rho^n}{r_f^{2n}+\rho^{2n}}, \\ H_{r--}^f &= -\frac{1}{2M'}\left[\partial_{r_f}^2 + \frac{1}{r_f}\partial_{r_f} - \frac{1}{r_f^2}\left(m_-^f - \frac{n\rho^{2n}}{r_f^{2n}+\rho^{2n}}\right)^2\right], \end{aligned} \tag{4.37}$$

while the rotational skyrmion contributions are given by

$$\begin{aligned} H_{r++++}^\gamma &= \frac{n^2}{2\mathcal{D}(\rho)\rho^2}\left(m + \sigma n\frac{\Theta}{2\pi} - 1 - \frac{\rho^{2n}}{r_\alpha^{2n}+\rho^{2n}} - \frac{\rho^{2n}}{r_\beta^{2n}+\rho^{2n}}\right)^2, \\ H_{r+-+-}^\gamma &= \frac{n^2}{2\mathcal{D}(\rho)\rho^2}\left(m + \sigma n\frac{\Theta}{2\pi} - \frac{\rho^{2n}}{r_\alpha^{2n}+\rho^{2n}} + \frac{\rho^{2n}}{r_\beta^{2n}+\rho^{2n}}\right)^2, \\ H_{r-+-+}^\gamma &= \frac{n^2}{2\mathcal{D}(\rho)\rho^2}\left(m + \sigma n\frac{\Theta}{2\pi} + \frac{\rho^{2n}}{r_\alpha^{2n}+\rho^{2n}} - \frac{\rho^{2n}}{r_\beta^{2n}+\rho^{2n}}\right)^2, \\ H_{r----}^\gamma &= \frac{n^2}{2\mathcal{D}(\rho)\rho^2}\left(m + \sigma n\frac{\Theta}{2\pi} + 1 + \frac{\rho^{2n}}{r_\alpha^{2n}+\rho^{2n}} + \frac{\rho^{2n}}{r_\beta^{2n}+\rho^{2n}}\right)^2. \end{aligned} \tag{4.38}$$

E. Symmetry properties of a pair of holes with different flavors localized on a skyrmion

It is worth noticing that the spin operator I, which commutes with the two-hole Hamiltonian H, is given by

$$I = \begin{pmatrix} -i\sigma\partial_\gamma + \sigma n\frac{\Theta}{2\pi} + 1 & 0 & 0 & 0 \\ 0 & -i\sigma\partial_\gamma + \sigma n\frac{\Theta}{2\pi} & 0 & 0 \\ 0 & 0 & -i\sigma\partial_\gamma + \sigma n\frac{\Theta}{2\pi} & 0 \\ 0 & 0 & 0 & -i\sigma\partial_\gamma + \sigma n\frac{\Theta}{2\pi} - 1 \end{pmatrix}, \tag{4.39}$$

such that

$$I\,\Psi^{\alpha\beta}_{\sigma,m_+^\alpha,m_-^\alpha,m_+^\beta,m_-^\beta,m}(r_\alpha,\chi_\alpha,r_\beta,\chi_\beta,\gamma) = \left(m + \sigma n\frac{\Theta}{2\pi}\right)\Psi^{\alpha\beta}_{\sigma,m_+^\alpha,m_-^\alpha,m_+^\beta,m_-^\beta,m}(r_\alpha,\chi_\alpha,r_\beta,\chi_\beta,\gamma). \tag{4.40}$$

Since m is an integer, as expected, for $\Theta = 0$ the state with two holes localized on a skyrmion has integer spin (which plays the role of "isospin").

The symmetries D_i', O, and R act on a general two-hole wave function

$$\Psi^{\alpha\beta}_{\sigma,n}(r_\alpha,\chi_\alpha,r_\beta,\chi_\beta,\gamma) = \begin{pmatrix} \Psi^{\alpha\beta}_{\sigma,n,++}(r_\alpha,\chi_\alpha,r_\beta,\chi_\beta,\gamma) \\ \Psi^{\alpha\beta}_{\sigma,n,+-}(r_\alpha,\chi_\alpha,r_\beta,\chi_\beta,\gamma) \\ \Psi^{\alpha\beta}_{\sigma,n,-+}(r_\alpha,\chi_\alpha,r_\beta,\chi_\beta,\gamma) \\ \Psi^{\alpha\beta}_{\sigma,n,--}(r_\alpha,\chi_\alpha,r_\beta,\chi_\beta,\gamma) \end{pmatrix} \tag{4.41}$$

as follows:

$$\begin{aligned}
{}^{D_i'}\Psi^{\alpha\beta}_{\sigma,n}(r_\alpha,\chi_\alpha,r_\beta,\chi_\beta,\gamma) &= \exp\left[i\left(k_i^\alpha + k_i^\beta\right)a\right]\begin{pmatrix} \Psi^{\alpha\beta}_{\sigma,n,--}(r_\alpha,\chi_\alpha,r_\beta,\chi_\beta,\gamma) \\ -\Psi^{\alpha\beta}_{\sigma,n,-+}(r_\alpha,\chi_\alpha,r_\beta,\chi_\beta,\gamma) \\ -\Psi^{\alpha\beta}_{\sigma,n,+-}(r_\alpha,\chi_\alpha,r_\beta,\chi_\beta,\gamma) \\ \Psi^{\alpha\beta}_{\sigma,n,++}(r_\alpha,\chi_\alpha,r_\beta,\chi_\beta,\gamma) \end{pmatrix}, \\
{}^{O}\Psi^{\alpha\beta}_{\sigma,n}(r_\alpha,\chi_\alpha,r_\beta,\chi_\beta,\gamma) &= \begin{pmatrix} -\Psi^{\alpha\beta}_{\sigma,n,++}(r_\beta,\chi_\beta+\frac{\pi}{2},r_\alpha,\chi_\alpha+\frac{\pi}{2},\gamma-n\frac{\pi}{2}) \\ -\Psi^{\alpha\beta}_{\sigma,n,-+}(r_\beta,\chi_\beta+\frac{\pi}{2},r_\alpha,\chi_\alpha+\frac{\pi}{2},\gamma-n\frac{\pi}{2}) \\ \Psi^{\alpha\beta}_{\sigma,n,+-}(r_\beta,\chi_\beta+\frac{\pi}{2},r_\alpha,\chi_\alpha+\frac{\pi}{2},\gamma-n\frac{\pi}{2}) \\ \Psi^{\alpha\beta}_{\sigma,n,--}(r_\beta,\chi_\beta+\frac{\pi}{2},r_\alpha,\chi_\alpha+\frac{\pi}{2},\gamma-n\frac{\pi}{2}) \end{pmatrix}, \\
{}^{R}\Psi^{\alpha\beta}_{\sigma,n}(r_\alpha,\chi_\alpha,r_\beta,\chi_\beta,\gamma) &= \begin{pmatrix} \Psi^{\alpha\beta}_{\sigma,n,++}(r_\beta,-\chi_\beta,r_\alpha,-\chi_\alpha,-\gamma) \\ \Psi^{\alpha\beta}_{\sigma,n,-+}(r_\beta,-\chi_\beta,r_\alpha,-\chi_\alpha,-\gamma) \\ \Psi^{\alpha\beta}_{\sigma,n,+-}(r_\beta,-\chi_\beta,r_\alpha,-\chi_\alpha,-\gamma) \\ \Psi^{\alpha\beta}_{\sigma,n,--}(r_\beta,-\chi_\beta,r_\alpha,-\chi_\alpha,-\gamma) \end{pmatrix}.
\end{aligned} \tag{4.42}$$

It is straightforward to show that for the two-hole energy eigenstates, this implies

$$\begin{aligned}
{}^{D_1'}\Psi^{\alpha\beta}_{\sigma,m_+^\alpha,m_-^\alpha,m_+^\beta,m_-^\beta,m}(r_\alpha,\chi_\alpha,r_\beta,\chi_\beta,\gamma) &= \Psi^{\alpha\beta}_{-\sigma,-m_-^\alpha,-m_+^\alpha,-m_-^\beta,-m_+^\beta,-m}(r_\alpha,\chi_\alpha,r_\beta,\chi_\beta,\gamma), \\
{}^{D_2'}\Psi^{\alpha\beta}_{\sigma,m_+^\alpha,m_-^\alpha,m_+^\beta,m_-^\beta,m}(r_\alpha,\chi_\alpha,r_\beta,\chi_\beta,\gamma) &= -\Psi^{\alpha\beta}_{-\sigma,-m_-^\alpha,-m_+^\alpha,-m_-^\beta,-m_+^\beta,-m}(r_\alpha,\chi_\alpha,r_\beta,\chi_\beta,\gamma), \\
{}^{O}\Psi^{\alpha\beta}_{\sigma,m_+^\alpha,m_-^\alpha,m_+^\beta,m_-^\beta,m}(r_\alpha,\chi_\alpha,r_\beta,\chi_\beta,\gamma) &= \exp\left(i\sigma[m_+^\alpha + m_-^\beta - mn + 1]\frac{\pi}{2}\right)\Psi^{\alpha\beta}_{\sigma,m_+^\alpha,m_-^\alpha,m_+^\beta,m_-^\beta,m}(r_\alpha,\chi_\alpha,r_\beta,\chi_\beta,\gamma), \\
{}^{R}\Psi^{\alpha\beta}_{\sigma,m_+^\alpha,m_-^\alpha,m_+^\beta,m_-^\beta,m}(r_\alpha,\chi_\alpha,r_\beta,\chi_\beta,\gamma) &= \Psi^{\alpha\beta}_{-\sigma,m_+^\beta,m_-^\beta,m_+^\alpha,m_-^\alpha,m}(r_\alpha,\chi_\alpha,r_\beta,\chi_\beta,\gamma).
\end{aligned} \tag{4.43}$$

Here, we have assumed an appropriate phase convention for the radial wave function $\psi_{\sigma,m_+^\alpha,m_-^\alpha,m_+^\beta,m_-^\beta,m}(r_\alpha,r_\beta)$. In the context of the shift symmetries D_i', we have used

$$\begin{aligned}
\psi_{\sigma,m_+^\alpha,m_-^\alpha,m_+^\beta,m_-^\beta,m,--}(r_\alpha,r_\beta) &= \psi_{-\sigma,-m_-^\alpha,-m_+^\alpha,-m_-^\beta,-m_+^\beta,-m,++}(r_\alpha,r_\beta), \\
\psi_{\sigma,m_+^\alpha,m_-^\alpha,m_+^\beta,m_-^\beta,m,-+}(r_\alpha,r_\beta) &= \psi_{-\sigma,-m_-^\alpha,-m_+^\alpha,-m_-^\beta,-m_+^\beta,-m,+-}(r_\alpha,r_\beta), \\
\psi_{\sigma,m_+^\alpha,m_-^\alpha,m_+^\beta,m_-^\beta,m,+-}(r_\alpha,r_\beta) &= \psi_{-\sigma,-m_-^\alpha,-m_+^\alpha,-m_-^\beta,-m_+^\beta,-m,-+}(r_\alpha,r_\beta), \\
\psi_{\sigma,m_+^\alpha,m_-^\alpha,m_+^\beta,m_-^\beta,m,++}(r_\alpha,r_\beta) &= \psi_{-\sigma,-m_-^\alpha,-m_+^\alpha,-m_-^\beta,-m_+^\beta,-m,--}(r_\alpha,r_\beta).
\end{aligned} \tag{4.44}$$

These relations follow from the symmetries of the radial Schrödinger equation (4.33). Similarly, in the context of the rotation O, we have used

$$\begin{aligned}\psi_{\sigma,m_+^\alpha,m_-^\alpha,m_+^\beta,m_-^\beta,m,++}(r_\beta,r_\alpha) &= \psi_{\sigma,m_+^\beta,m_-^\beta,m_+^\alpha,m_-^\alpha,m,++}(r_\alpha,r_\beta),\\ \psi_{\sigma,m_+^\alpha,m_-^\alpha,m_+^\beta,m_-^\beta,m,-+}(r_\beta,r_\alpha) &= \psi_{\sigma,m_+^\beta,m_-^\beta,m_+^\alpha,m_-^\alpha,m,+-}(r_\alpha,r_\beta),\\ \psi_{\sigma,m_+^\alpha,m_-^\alpha,m_+^\beta,m_-^\beta,m,+-}(r_\beta,r_\alpha) &= \psi_{\sigma,m_+^\beta,m_-^\beta,m_+^\alpha,m_-^\alpha,m,-+}(r_\alpha,r_\beta),\\ \psi_{\sigma,m_+^\alpha,m_-^\alpha,m_+^\beta,m_-^\beta,m,--}(r_\beta,r_\alpha) &= \psi_{\sigma,m_+^\beta,m_-^\beta,m_+^\alpha,m_-^\alpha,m,--}(r_\alpha,r_\beta).\end{aligned} \tag{4.45}$$

Finally, in the context of the reflection symmetry R, we have used

$$\begin{aligned}\psi_{\sigma,m_+^\alpha,m_-^\alpha,m_+^\beta,m_-^\beta,m,++}(r_\beta,r_\alpha) &= \psi_{-\sigma,m_+^\beta,m_-^\beta,m_+^\alpha,m_-^\alpha,m,++}(r_\alpha,r_\beta),\\ \psi_{\sigma,m_+^\alpha,m_-^\alpha,m_+^\beta,m_-^\beta,m,-+}(r_\beta,r_\alpha) &= \psi_{-\sigma,m_+^\beta,m_-^\beta,m_+^\alpha,m_-^\alpha,m,+-}(r_\alpha,r_\beta),\\ \psi_{\sigma,m_+^\alpha,m_-^\alpha,m_+^\beta,m_-^\beta,m,+-}(r_\beta,r_\alpha) &= \psi_{-\sigma,m_+^\beta,m_-^\beta,m_+^\alpha,m_-^\alpha,m,-+}(r_\alpha,r_\beta),\\ \psi_{\sigma,m_+^\alpha,m_-^\alpha,m_+^\beta,m_-^\beta,m,--}(r_\beta,r_\alpha) &= \psi_{-\sigma,m_+^\beta,m_-^\beta,m_+^\alpha,m_-^\alpha,m,--}(r_\alpha,r_\beta).\end{aligned} \tag{4.46}$$

The relations in Eq. (4.46) follow from the symmetries of the radial Schrödinger equation (4.33) for $\Theta = 0$. For $\Theta \neq 0$ or π, the Hopf term explicitly breaks the reflection symmetry.

F. Comparison with two-hole states bound by one-magnon exchange

In Ref. 14, states of two holes bound by one-magnon exchange in a square lattice antiferromagnet have been investigated in great detail. Here, we summarize as well as extend some of the relevant results. In the rest frame, the Schrödinger equation for two holes of flavor α and β takes the form

$$\begin{pmatrix} -\frac{1}{M'}\Delta & V^{\alpha\beta}(\vec{r}) \\ V^{\alpha\beta}(\vec{r}) & -\frac{1}{M'}\Delta \end{pmatrix}\begin{pmatrix}\Psi_1(\vec{r})\\ \Psi_2(\vec{r})\end{pmatrix} = E\begin{pmatrix}\Psi_1(\vec{r})\\ \Psi_2(\vec{r})\end{pmatrix}. \tag{4.47}$$

The components $\Psi_1(\vec{r})$ and $\Psi_2(\vec{r})$ are probability amplitudes for the spin-flavor combinations $\alpha_+\beta_-$ and $\alpha_-\beta_+$, respectively. The potential

$$V^{\alpha\beta}(\vec{r}) = \frac{\Lambda^2}{2\pi\rho_s}\frac{\cos(2\varphi)}{r^2} \tag{4.48}$$

couples the two channels because magnon exchange is accompanied by a spin flip. Here, $\vec{r} = \vec{r}_+ - \vec{r}_-$ is the distance vector between the two holes of spin $+$ and $-$ and φ is the angle between $\vec{r}$ and the x axis. Magnon exchange is attractive between holes of opposite spin, and hence magnon-mediated two-hole bound states are invariant under the unbroken subgroup $U(1)_s$. We make the ansatz

$$\Psi_1(\vec{r}) \pm \Psi_2(\vec{r}) = R(r)\chi_\pm(\varphi). \tag{4.49}$$

For the angular part of the wave function, this implies

$$-\frac{d^2\chi_\pm(\varphi)}{d\varphi^2} \pm \frac{M'\Lambda^2}{2\pi\rho_s}\cos(2\varphi)\chi_\pm(\varphi) = -\lambda\chi_\pm(\varphi). \tag{4.50}$$

This is a Mathieu equation, the solution with the lowest eigenvalue $-\lambda_1$ of which is given by

$$\begin{aligned}\chi_\pm^1(\varphi) &= \frac{1}{\sqrt{\pi}}\mathrm{ce}_0\left(\varphi, \pm\frac{M'\Lambda^2}{4\pi\rho_s}\right),\\ \lambda_1 &= \frac{1}{2}\left(\frac{M'\Lambda^2}{4\pi\rho_s}\right)^2 + \mathcal{O}(\Lambda^8).\end{aligned} \tag{4.51}$$

The first excited state and its eigenvalue $-\lambda_2$ is given by

$$\begin{aligned}\chi_+^2(\varphi) &= \frac{1}{\sqrt{\pi}}\mathrm{se}_1\left(\varphi, \frac{M'\Lambda^2}{4\pi\rho_s}\right),\\ \chi_-^2(\varphi) &= \frac{1}{\sqrt{\pi}}\mathrm{se}_1\left(\varphi - \frac{\pi}{2}, \frac{M'\Lambda^2}{4\pi\rho_s}\right)\\ &= -\frac{1}{\sqrt{\pi}}\mathrm{ce}_1\left(\varphi, -\frac{M'\Lambda^2}{4\pi\rho_s}\right),\\ \lambda_2 &= -1 + \frac{M'\Lambda^2}{4\pi\rho_s} + \frac{1}{8}\left(\frac{M'\Lambda^2}{4\pi\rho_s}\right)^2\\ &\quad - \frac{1}{64}\left(\frac{M'\Lambda^2}{4\pi\rho_s}\right)^3 + \mathcal{O}(\Lambda^8).\end{aligned} \tag{4.52}$$

For small Λ, $\lambda_2 < 0$, which (as we will see) implies that the corresponding two-hole state is unbound. For $M'\Lambda^2/4\pi\rho_s > 0.908\,046$, on the other hand, $\lambda_1,\lambda_2 > 0$, such that then both states are bound. The periodic Mathieu functions $\mathrm{ce}_0(\varphi, M'\Lambda^2/4\pi\rho_s)$ and $\mathrm{se}_1(\varphi, M'\Lambda^2/4\pi\rho_s)$ (Ref. 64) are shown in Fig. 3. The corresponding radial Schrödinger equation is given by

$$\begin{aligned}-\left[\frac{d^2R_i(r)}{dr^2} + \frac{1}{r}\frac{dR_i(r)}{dr}\right] - \frac{\lambda_i}{r^2}R_i(r)\\ = M'E_iR_i(r), \quad i \in \{1,2\}.\end{aligned} \tag{4.53}$$

The short-distance repulsion between two holes can be incorporated by a hard core of radius r_0, i.e., we require $R_i(r_0) = 0$. The radial Schrödinger equation for the bound states is solved by a Bessel function

$$R_i(r) = A_iK_\nu(\sqrt{M'|E_{ik}|}r), \quad k = 1,2,3,\ldots, \quad \nu = i\sqrt{\lambda_i}. \tag{4.54}$$

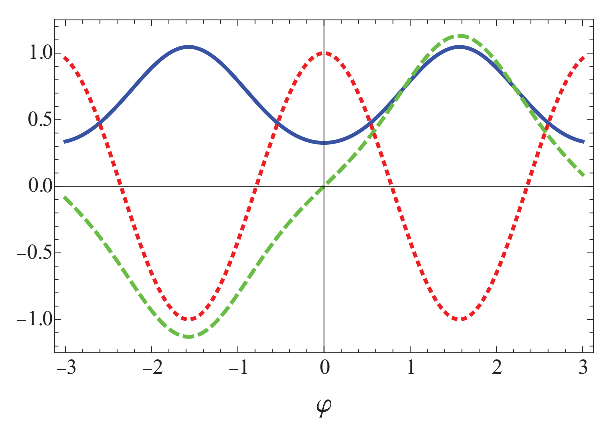

FIG. 3. (Color online) Angular wave functions $\mathrm{ce}_0(\varphi, M'\Lambda^2/4\pi\rho_s)$ (solid curve) and $\mathrm{se}_1(\varphi, M'\Lambda^2/4\pi\rho_s)$ (dashed curve) as well as the angle dependence $\cos(2\varphi)$ of the potential (dotted curve) for a pair of holes with flavors α and β ($M'\Lambda^2/4\pi\rho_s = 1.25$).

The energy [determined from $K_\nu(\sqrt{M'|E_{ik}|}r_0) = 0$] is then given by

$$E_{ik} \sim -\left(M' r_0^2\right)^{-1} \exp(-2\pi k/\sqrt{\lambda_i}) \tag{4.55}$$

for large n. Magnon exchange mediates weak attractive forces that lead to a small binding energy.

The two lowest-energy states with angular part $\chi_+^1(\varphi)$ and $\chi_-^1(\varphi)$ are degenerate in energy. By linearly combining the two states to two eigenstates of the rotation O, one obtains

$$\Psi_\pm^1(\vec{r}) = R_1(r)\begin{pmatrix} \chi_+^1(\varphi) \mp i\chi_-^1(\varphi) \\ \chi_+^1(\varphi) \pm i\chi_-^1(\varphi) \end{pmatrix}. \tag{4.56}$$

The corresponding probability density is illustrated in Fig. 4 (left panel). While the probability density seems to resemble $d_{x^2-y^2}$ symmetry, unlike for an actual d wave, the wave function is suppressed, but not equal to zero, along the lattice diagonals. In fact, as one operates on the states $\Psi_\pm^1(\vec{r})$ with the 90° rotation O, one obtains the eigenvalues $\pm i$, which show that they actually have p-wave symmetry.

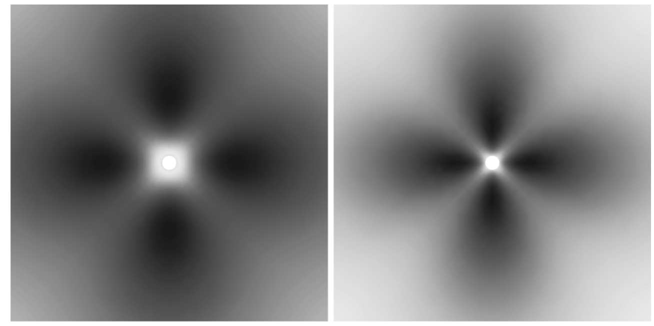

FIG. 4. Probability distribution for two holes with flavors α and β. Left panel: the ground state with p-wave symmetry. Right panel: excited states with s- or d-wave symmetry, but with identical probability densities ($M'\Lambda^2/4\pi\rho_s = 1.25$, $r_0 = a$).

Under the discrete symmetries D_i', O, and R, the ground states $\Psi_\pm^1(\vec{r})$, which are bound by magnon exchange, transform as

$$\begin{aligned}
{}^{D_1'}\Psi_\pm^1(\vec{r}) &= R_1(r)\begin{pmatrix} \chi_+^1(\varphi) \pm i\chi_-^1(\varphi) \\ \chi_+^1(\varphi) \mp i\chi_-^1(\varphi) \end{pmatrix} = \Psi_\mp^1(\vec{r}),\\
{}^{D_2'}\Psi_\pm^1(\vec{r}) &= -R_1(r)\begin{pmatrix} \chi_+^1(\varphi) \pm i\chi_-^1(\varphi) \\ \chi_+^1(\varphi) \mp i\chi_-^1(\varphi) \end{pmatrix} = -\Psi_\mp^1(\vec{r}),\\
{}^{O}\Psi_\pm^1(\vec{r}) &= R_1(r)\begin{pmatrix} \chi_+^1(\varphi+\frac{\pi}{2}) \pm i\chi_-^1(\varphi+\frac{\pi}{2}) \\ -\chi_+^1(\varphi+\frac{\pi}{2}) \pm i\chi_-^1(\varphi+\frac{\pi}{2}) \end{pmatrix} = R_1(r)\begin{pmatrix} \chi_-^1(\varphi) \pm i\chi_+^1(\varphi) \\ -\chi_-^1(\varphi) \pm i\chi_+^1(\varphi) \end{pmatrix} = \pm i\Psi_\pm^1(\vec{r}),\\
{}^{R}\Psi_\pm^1(\vec{r}) &= R_1(r)\begin{pmatrix} \chi_+^1(-\varphi) \pm i\chi_-^1(-\varphi) \\ \chi_+^1(-\varphi) \mp i\chi_-^1(-\varphi) \end{pmatrix} = R_1(r)\begin{pmatrix} \chi_+^1(\varphi) \pm i\chi_-^1(\varphi) \\ \chi_+^1(\varphi) \mp i\chi_-^1(\varphi) \end{pmatrix} = \Psi_\mp^1(\vec{r}).
\end{aligned} \tag{4.57}$$

It should be noted that in Ref. 14 there are two typos in the last line of the previous equation for the reflection symmetry R [Eq. (6.20) in Ref. 14].

Remarkably, the magnon-mediated two-hole ground states $\Psi_\pm^1(\vec{r})$ transform exactly as the two-hole states localized on a rotating skyrmion with $n = 1$, provided that we associate $\Psi_\pm^1(\vec{r})$ with the corresponding two-hole-skyrmion wave function $\Psi^{\alpha\beta}_{\pm,-1,1,-1,1,0}(r_\alpha,\chi_\alpha,r_\beta,\chi_\beta,\gamma)$ with the quantum numbers $\sigma = \pm, m_+^\alpha = m_+^\beta = -1, m_-^\alpha = m_-^\beta = 1$, and $m = 0$. Indeed, according to Eq. (4.43), one obtains

$$\begin{aligned}
{}^{D_1'}\Psi^{\alpha\beta}_{\pm,-1,1,-1,1,0}(r_\alpha,\chi_\alpha,r_\beta,\chi_\beta,\gamma) &= \Psi^{\alpha\beta}_{\mp,-1,1,-1,1,0}(r_\alpha,\chi_\alpha,r_\beta,\chi_\beta,\gamma),\\
{}^{D_2'}\Psi^{\alpha\beta}_{\pm,-1,1,-1,1,0}(r_\alpha,\chi_\alpha,r_\beta,\chi_\beta,\gamma) &= -\Psi^{\alpha\beta}_{\mp,-1,1,-1,1,0}(r_\alpha,\chi_\alpha,r_\beta,\chi_\beta,\gamma),\\
{}^{O}\Psi^{\alpha\beta}_{\pm,-1,1,-1,1,0}(r_\alpha,\chi_\alpha,r_\beta,\chi_\beta,\gamma) &= \pm i\Psi^{\alpha\beta}_{\pm,-1,1,-1,1,0}(r_\alpha,\chi_\alpha,r_\beta,\chi_\beta,\gamma),\\
{}^{R}\Psi^{\alpha\beta}_{\pm,-1,1,-1,1,0}(r_\alpha,\chi_\alpha,r_\beta,\chi_\beta,\gamma) &= \Psi^{\alpha\beta}_{\mp,-1,1,-1,1,0}(r_\alpha,\chi_\alpha,r_\beta,\chi_\beta,\gamma).
\end{aligned} \tag{4.58}$$

Just as the magnon-mediated bound states, these states are also invariant under $U(1)_s$ and they have fermion number 2. One may argue that the two-hole-skyrmion states, in addition, have skyrmion number as a conserved topological quantum number. However, as we discussed before, skyrmion number has no analog in the underlying microscopic Hubbard or t-J models and is just an accidental symmetry of the effective theory. We thus conclude that, in their ground state, two holes bound by magnon exchange indeed have exactly the same quantum numbers as two holes localized on a rotating skyrmion with $n = 1$. This implies that these sets of states may evolve into each other upon doping. In this way, two holes weakly bound by magnon exchange at small doping may evolve into a strongly correlated preformed pair of holes localized on a skyrmion. However, as we have just seen, theses bound states actually have p-wave symmetry.

Let us also consider the excited states, bound by magnon exchange, with angular part $\chi^2_+(\varphi)$ and $\chi^2_-(\varphi)$, which are again degenerate. By linearly combining these two states to two eigenstates of the rotation O, one obtains

$$\Psi^2_\pm(\vec{r}) = R_2(r)\begin{pmatrix}\chi^2_+(\varphi) \mp \chi^2_-(\varphi)\\ \chi^2_+(\varphi) \pm \chi^2_-(\varphi)\end{pmatrix}. \tag{4.59}$$

Operating on the states $\Psi^2_\pm(\vec{r})$ with the 90° rotation O, one now obtains the eigenvalues ±1, which implies that $\Psi^2_+(\vec{r})$ represents an s wave, while $\Psi^2_-(\vec{r})$ actually has d-wave symmetry. As a consequence of an interplay of the various symmetries, the two states are exactly degenerate. The corresponding probability density is illustrated in Fig. 4 (right panel). Interestingly, although the states have different symmetries, their probability densities are identical.

Under the discrete symmetries D'_i, O, and R, the excited states $\Psi^2_\pm(\vec{r})$, which are bound by magnon exchange, transform as

$$\begin{aligned}
{}^{D'_1}\Psi^2_\pm(\vec{r}) &= -R_2(r)\begin{pmatrix}\chi^2_+(\varphi) \pm \chi^2_-(\varphi)\\ \chi^2_+(\varphi) \mp \chi^2_-(\varphi)\end{pmatrix} = -\Psi^2_\mp(\vec{r}),\\
{}^{D'_2}\Psi^2_\pm(\vec{r}) &= R_2(r)\begin{pmatrix}\chi^2_+(\varphi) \pm \chi^2_-(\varphi)\\ \chi^2_+(\varphi) \mp \chi^2_-(\varphi)\end{pmatrix} = \Psi^2_\mp(\vec{r}),\\
{}^{O}\Psi^2_\pm(\vec{r}) &= R_2(r)\begin{pmatrix}\chi^2_+\left(\varphi+\frac{\pi}{2}\right) \pm \chi^2_-\left(\varphi+\frac{\pi}{2}\right)\\ -\chi^2_+\left(\varphi+\frac{\pi}{2}\right) \pm \chi^2_-\left(\varphi+\frac{\pi}{2}\right)\end{pmatrix} = R_2(r)\begin{pmatrix}-\chi^2_-(\varphi) \pm \chi^2_+(\varphi)\\ \chi^2_-(\varphi) \pm \chi^2_+(\varphi)\end{pmatrix} = \pm\Psi^2_\pm(\vec{r}),\\
{}^{R}\Psi^2_\pm(\vec{r}) &= R_2(r)\begin{pmatrix}\chi^2_+(-\varphi) \pm \chi^2_-(-\varphi)\\ \chi^2_+(-\varphi) \mp \chi^2_-(-\varphi)\end{pmatrix} = R_2(r)\begin{pmatrix}-\chi^2_+(\varphi) \pm \chi^2_-(\varphi)\\ -\chi^2_+(\varphi) \mp \chi^2_-(\varphi)\end{pmatrix} = -\Psi^2_\pm(\vec{r}).
\end{aligned} \tag{4.60}$$

States with d-wave symmetry can also be constructed for two holes localized on a skyrmion. For example, for $n = 1$, the states $\Psi^{\alpha\beta}_{\pm,-1,1,0,2,0}(r_\alpha,\chi_\alpha,r_\beta,\chi_\beta,\gamma)$ and $\Psi^{\alpha\beta}_{\pm,0,2,-1,1,0}(r_\alpha,\chi_\alpha,r_\beta,\chi_\beta,\gamma)$ have d-wave symmetry. Under the symmetries D'_1 and D'_2, they transform into $\Psi^{\alpha\beta}_{\mp,-1,1,-2,0,0}(r_\alpha,\chi_\alpha,r_\beta,\chi_\beta,\gamma)$ and $\Psi^{\alpha\beta}_{\mp,-2,0,-1,1,0}(r_\alpha,\chi_\alpha,r_\beta,\chi_\beta,\gamma)$, which have s-wave symmetry. According to Eq. (4.43), under the various symmetries the d-wave states transform as

$$\begin{aligned}
{}^{D'_1}\Psi^{\alpha\beta}_{\pm,-1,1,0,2,0}(r_\alpha,\chi_\alpha,r_\beta,\chi_\beta,\gamma) &= \Psi^{\alpha\beta}_{\mp,-1,1,-2,0,0}(r_\alpha,\chi_\alpha,r_\beta,\chi_\beta,\gamma),\\
{}^{D'_2}\Psi^{\alpha\beta}_{\pm,-1,1,0,2,0}(r_\alpha,\chi_\alpha,r_\beta,\chi_\beta,\gamma) &= -\Psi^{\alpha\beta}_{\mp,-1,1,-2,0,0}(r_\alpha,\chi_\alpha,r_\beta,\chi_\beta,\gamma),\\
{}^{O}\Psi^{\alpha\beta}_{\pm,-1,1,0,2,0}(r_\alpha,\chi_\alpha,r_\beta,\chi_\beta,\gamma) &= -\Psi^{\alpha\beta}_{\pm,-1,1,0,2,0}(r_\alpha,\chi_\alpha,r_\beta,\chi_\beta,\gamma),\\
{}^{R}\Psi^{\alpha\beta}_{\pm,-1,1,0,2,0}(r_\alpha,\chi_\alpha,r_\beta,\chi_\beta,\gamma) &= \Psi^{\alpha\beta}_{\mp,0,2,-1,1,0}(r_\alpha,\chi_\alpha,r_\beta,\chi_\beta,\gamma),\\
{}^{D'_1}\Psi^{\alpha\beta}_{\pm,0,2,-1,1,0}(r_\alpha,\chi_\alpha,r_\beta,\chi_\beta,\gamma) &= \Psi^{\alpha\beta}_{\mp,-2,0,-1,1,0}(r_\alpha,\chi_\alpha,r_\beta,\chi_\beta,\gamma),\\
{}^{D'_2}\Psi^{\alpha\beta}_{\pm,0,2,-1,1,0}(r_\alpha,\chi_\alpha,r_\beta,\chi_\beta,\gamma) &= -\Psi^{\alpha\beta}_{\mp,-2,0,-1,1,0}(r_\alpha,\chi_\alpha,r_\beta,\chi_\beta,\gamma),\\
{}^{O}\Psi^{\alpha\beta}_{\pm,0,2,-1,1,0}(r_\alpha,\chi_\alpha,r_\beta,\chi_\beta,\gamma) &= -\Psi^{\alpha\beta}_{\pm,0,2,-1,1,0}(r_\alpha,\chi_\alpha,r_\beta,\chi_\beta,\gamma),\\
{}^{R}\Psi^{\alpha\beta}_{\pm,0,2,-1,1,0}(r_\alpha,\chi_\alpha,r_\beta,\chi_\beta,\gamma) &= \Psi^{\alpha\beta}_{\mp,-1,1,0,2,0}(r_\alpha,\chi_\alpha,r_\beta,\chi_\beta,\gamma).
\end{aligned} \tag{4.61}$$

Similarly, the s-wave states transform as follows:

$$\begin{aligned}
{}^{D'_1}\Psi^{\alpha\beta}_{\pm,-1,1,-2,0,0}(r_\alpha,\chi_\alpha,r_\beta,\chi_\beta,\gamma) &= \Psi^{\alpha\beta}_{\mp,-1,1,0,2,0}(r_\alpha,\chi_\alpha,r_\beta,\chi_\beta,\gamma),\\
{}^{D'_2}\Psi^{\alpha\beta}_{\pm,-1,1,-2,0,0}(r_\alpha,\chi_\alpha,r_\beta,\chi_\beta,\gamma) &= -\Psi^{\alpha\beta}_{\mp,-1,1,0,2,0}(r_\alpha,\chi_\alpha,r_\beta,\chi_\beta,\gamma),\\
{}^{O}\Psi^{\alpha\beta}_{\pm,-1,1,-2,0,0}(r_\alpha,\chi_\alpha,r_\beta,\chi_\beta,\gamma) &= \Psi^{\alpha\beta}_{\pm,-1,1,-2,0,0}(r_\alpha,\chi_\alpha,r_\beta,\chi_\beta,\gamma),\\
{}^{R}\Psi^{\alpha\beta}_{\pm,-1,1,-2,0,0}(r_\alpha,\chi_\alpha,r_\beta,\chi_\beta,\gamma) &= \Psi^{\alpha\beta}_{\mp,-2,0,-1,1,0}(r_\alpha,\chi_\alpha,r_\beta,\chi_\beta,\gamma),\\
{}^{D'_1}\Psi^{\alpha\beta}_{\pm,-2,0,-1,1,0}(r_\alpha,\chi_\alpha,r_\beta,\chi_\beta,\gamma) &= \Psi^{\alpha\beta}_{\mp,0,2,-1,1,0}(r_\alpha,\chi_\alpha,r_\beta,\chi_\beta,\gamma),\\
{}^{D'_2}\Psi^{\alpha\beta}_{\pm,-2,0,-1,1,0}(r_\alpha,\chi_\alpha,r_\beta,\chi_\beta,\gamma) &= -\Psi^{\alpha\beta}_{\mp,0,2,-1,1,0}(r_\alpha,\chi_\alpha,r_\beta,\chi_\beta,\gamma),\\
{}^{O}\Psi^{\alpha\beta}_{\pm,-2,0,-1,1,0}(r_\alpha,\chi_\alpha,r_\beta,\chi_\beta,\gamma) &= \Psi^{\alpha\beta}_{\pm,-2,0,-1,1,0}(r_\alpha,\chi_\alpha,r_\beta,\chi_\beta,\gamma),\\
{}^{R}\Psi^{\alpha\beta}_{\pm,-2,0,-1,1,0}(r_\alpha,\chi_\alpha,r_\beta,\chi_\beta,\gamma) &= \Psi^{\alpha\beta}_{\mp,-1,1,-2,0,0}(r_\alpha,\chi_\alpha,r_\beta,\chi_\beta,\gamma).
\end{aligned} \tag{4.62}$$

Hence, just as for the magnon-mediated excited states, as a consequence of the interplay of the various symmetries, s- and d-wave states are again degenerate.

Alternatively, d-wave states also arise for two holes localized on a skyrmion with winding number $n = 2$. For example, the two states $\Psi^{\alpha\beta}_{\pm,-1,2,-1,2,0}(r_\alpha,\chi_\alpha,r_\beta,\chi_\beta,\gamma)$ have d-wave symmetry, and they transform into the states $\Psi^{\alpha\beta}_{\mp,-2,1,-2,1,0}(r_\alpha,\chi_\alpha,r_\beta,\chi_\beta,\gamma)$, which again have s-wave symmetry, under D_1' and D_2'. According to Eq. (4.43), the d-wave states transform as

$$\begin{aligned}
{}^{D_1'}\Psi^{\alpha\beta}_{\pm,-1,2,-1,2,0}(r_\alpha,\chi_\alpha,r_\beta,\chi_\beta,\gamma) &= \Psi^{\alpha\beta}_{\mp,-2,1,-2,1,0}(r_\alpha,\chi_\alpha,r_\beta,\chi_\beta,\gamma),\\
{}^{D_2'}\Psi^{\alpha\beta}_{\pm,-1,2,-1,2,0}(r_\alpha,\chi_\alpha,r_\beta,\chi_\beta,\gamma) &= -\Psi^{\alpha\beta}_{\mp,-2,1,-2,1,0}(r_\alpha,\chi_\alpha,r_\beta,\chi_\beta,\gamma),\\
{}^{O}\Psi^{\alpha\beta}_{\pm,-1,2,-1,2,0}(r_\alpha,\chi_\alpha,r_\beta,\chi_\beta,\gamma) &= -\Psi^{\alpha\beta}_{\pm,-1,2,-1,2,0}(r_\alpha,\chi_\alpha,r_\beta,\chi_\beta,\gamma),\\
{}^{R}\Psi^{\alpha\beta}_{\pm,-1,2,-1,2,0}(r_\alpha,\chi_\alpha,r_\beta,\chi_\beta,\gamma) &= \Psi^{\alpha\beta}_{\mp,-1,2,-1,2,0}(r_\alpha,\chi_\alpha,r_\beta,\chi_\beta,\gamma),
\end{aligned} \tag{4.63}$$

while the s-wave states transform as

$$\begin{aligned}
{}^{D_1'}\Psi^{\alpha\beta}_{\pm,-2,1,-2,1,0}(r_\alpha,\chi_\alpha,r_\beta,\chi_\beta,\gamma) &= \Psi^{\alpha\beta}_{\mp,-1,2,-1,2,0}(r_\alpha,\chi_\alpha,r_\beta,\chi_\beta,\gamma),\\
{}^{D_2'}\Psi^{\alpha\beta}_{\pm,-2,1,-2,1,0}(r_\alpha,\chi_\alpha,r_\beta,\chi_\beta,\gamma) &= -\Psi^{\alpha\beta}_{\mp,-1,2,-1,2,0}(r_\alpha,\chi_\alpha,r_\beta,\chi_\beta,\gamma),\\
{}^{O}\Psi^{\alpha\beta}_{\pm,-2,1,-2,1,0}(r_\alpha,\chi_\alpha,r_\beta,\chi_\beta,\gamma) &= \Psi^{\alpha\beta}_{\pm,-2,1,-2,1,0}(r_\alpha,\chi_\alpha,r_\beta,\chi_\beta,\gamma),\\
{}^{R}\Psi^{\alpha\beta}_{\pm,-2,1,-2,1,0}(r_\alpha,\chi_\alpha,r_\beta,\chi_\beta,\gamma) &= \Psi^{\alpha\beta}_{\mp,-2,1,-2,1,0}(r_\alpha,\chi_\alpha,r_\beta,\chi_\beta,\gamma).
\end{aligned} \tag{4.64}$$

Depending on the details of the dynamics, the investigation of which goes beyond the scope of this paper, it may be possible that the degenerate s- and d-wave states have a lower energy than the p-wave states discussed earlier.

G. Possible implications for Cooper-pair formation in high-temperature superconductors

As we have seen, two holes, one of flavor α and one of flavor β, can both get localized in the ground state of a single rotating skyrmion with $n = 1$, which turns out to have p-wave symmetry. Alternatively, the holes may get localized on a rotating $n = 1$ or 2 skyrmion with s- or d-wave symmetry. As discussed in the Appendix, two holes of the same flavor can also get localized on a skyrmion. It will be the subject of a subsequent publication to decide which of the various states is energetically most favorable.

While in this paper we have concentrated on a detailed symmetry analysis, we also want to get at least a crude estimate of the binding energy of two-hole states localized on an $n = 1$ skyrmion. Ignoring contact interactions between the two holes, the total energy of the bound state of two holes and a skyrmion can then be estimated as

$$E_{\text{tot}} = 2M + 4\pi\rho_s + 2E_0, \tag{4.65}$$

while two free holes (not localized on a skyrmion) just have their rest energy $2M$. Using the result of Eq. (4.13), the perturbative ground state thus becomes unstable against the formation of two-hole-skyrmion bound states when

$$4\pi\rho_s + 2E_0 < 0 \;\Rightarrow\; 0.270M'\Lambda^2 > 4\pi\rho_s. \tag{4.66}$$

Hence, for sufficiently small spin stiffness ρ_s, the instability will indeed arise. Similar instabilities are related to the formation of spiral phases in the staggered magnetization order parameter. In particular, in Ref. 25 we have shown that the ground state with a spatially constant staggered magnetization becomes unstable against the formation of a 45° spiral phase for $M'\Lambda^2 > 4\pi\rho_s$. Since antiferromagnetism is weakened upon doping, ρ_s is expected to eventually go to zero. Before this happens, pairs of holes will get localized on a skyrmion.

In order to get at least a rough idea of the involved energy scales, let us estimate the values of the relevant low-energy parameters for realistic lightly doped quantum antiferromagnets. By comparison with Refs. 23, 26 and 27, where a generalized t-J model on a square lattice with spacing a was considered at $J/t \approx 0.3$, one obtains the rough estimate

$$M' \approx \frac{1}{ta^2} \approx \frac{0.3}{Ja^2}, \quad \Lambda \approx 2.5Ja. \tag{4.67}$$

It would be interesting and definitely feasible to extract these parameters with high precision from numerical simulations. In this way, in the Heisenberg model (i.e., the undoped t-J model), very accurate numerical results have been obtained for the spin stiffness, the spin-wave velocity, and the staggered magnetization per lattice site:[1,3,4]

$$\rho_s = 0.18081(11)J, \;\; c = 1.6586(3)Ja, \;\; \mathcal{M}_s = 0.30743(1)/a^2. \tag{4.68}$$

Hence, one obtains $0.270M'\Lambda^2 \approx 0.5J$ compared to $4\pi\rho_s = 2.2721(1)J$, which implies that two-hole-skyrmion bound states are still far from being energetically favorable at zero doping. The exchange coupling of undoped La_2CuO_4 is $J = 1540(60)$ K.[1] A high transition temperature of $T_c \approx 50$ K, and hence $T_c \approx 0.03J$, would thus require a two-hole-skyrmion bound-state energy of about

$$4\pi\rho_s + 2E_0 = 4\pi\rho_s - 0.270M'\Lambda^2 \approx -0.03J \Rightarrow \rho_s \approx 0.04J. \tag{4.69}$$

If doping reduces ρ_s by a factor of about 4 or 5 (and assuming for simplicity that the other parameters remain unchanged), the estimated energy scales should indeed be of the right magnitude in order to make two holes localized on a rotating skyrmion a viable candidate for a preformed Cooper pair of a high-temperature superconductor. Using Eq. (4.12), one can estimate the radius of the skyrmion, which sets the scale for the size of the candidate Cooper pair, as $\rho \approx 1/(0.271M'\Lambda) \approx 5a$, which again seems reasonable.

It may involve some wishful thinking to assume that the d-wave state of two holes localized on an $n = 1$ or 2 skyrmion will not only turn out to be energetically favorable, but also ready to condense at sufficiently large doping. However, we think that it is worthwhile to take this possibility seriously. Deciding whether the radial dynamics favors these states as promising candidates for a preformed Cooper pair in the pseudogap phase is the natural next step. The question of condensation is another important issue.

V. CONCLUSIONS

We have performed a detailed study of the localization of holes on a skyrmion in a square lattice antiferromagnet. When two holes get localized on the same skyrmion, they form a bound state. Interestingly, in some cases, the quantum numbers of these topologically nontrivial bound states are the same as those of the topologically trivial bound states resulting from one-magnon exchange between two holes. The ground state of two holes weakly bound by one-magnon exchange has p-wave symmetry and may evolve into a strongly bound state of two holes localized on an $n = 1$ skyrmion at strong coupling.

Magnon-mediated two-hole bound states which are excited in the angular motion have s- or d-wave symmetry. Remarkably, s- and d-wave states are degenerate due to an interplay of the various symmetries. Similarly, there are strongly bound states of two holes localized on an $n = 1$ or 2 skyrmion which also have s- or d-wave symmetry, and are again degenerate. Which of these states is energetically most favorable will be an interesting subject for future studies. If a d-wave state turns out to be the ground state at sufficiently strong doping, two holes localized on a skyrmion are a promising candidate for a preformed Cooper pair in the pseudogap regime. Interestingly, the effective theory provides detailed predictions for the anatomy of these objects. In particular, their angular structure follows unambiguously from our symmetry analysis, and is insensitive to the details of the radial dynamics.

Understanding the dynamical mechanism responsible for high-temperature superconductivity has proved to be one of the most challenging problems in theoretical physics. While hole-pair localization on a rotating skyrmion may ultimately turn out not to be the relevant mechanism, it seems rather promising. Beyond the symmetry analysis presented here, studying its dynamics in more detail is certainly worthwhile.

ACKNOWLEDGMENTS

We like to thank C. Brügger and F. Kämpfer for contributing to the early stages of the work reported here. U.-J.W. likes to thank P. A. Lee and F. Wilczek for discussions and encouragement at the beginning of the project. C.P.H., F.-J.J., and N.D.V. thank the Institute for Theoretical Physics at Bern University for warm hospitality. C.P.H. gratefully acknowledges financial support from the Universidad de Colima. F.-J.J. is partially supported by NSC and NCTS (North) of Taiwan. This work is supported by funds provided by the Schweizerischer Nationalfonds (SNF). In the early phases of this work, N.D.V. was supported through an SNF SCOPES grant. The Albert Einstein Center for Fundamental Physics at Bern University is supported by the "Innovations- und Kooperationsprojekt C-13" of the Schweizerische Universitätskonferenz (SUK/CRUS).

APPENDIX: HOLE PAIRS OF THE SAME FLAVOR

In this Appendix, we consider a pair of holes in a square lattice antiferromagnet residing in the same hole pocket. First, we investigate two holes localized on a rotating skyrmion, and then we compare the results with the corresponding two-hole magnon-mediated bound states.

1. Schrödinger equation for a pair of holes of the same flavor localized on a rotating skyrmion

Let us consider bound states of two holes of the same flavor f localized on a rotating skyrmion. In this case, as a consequence of the Pauli principle, the holes can not occupy the same quantum state. We distinguish the holes by an unphysical label 1 or 2. In order to satisfy the Pauli principle, the wave function must be antisymmetric under the exchange of the two labels.

The Hamiltonian for two holes of the same flavor f is then given by

$$H = H^1 + H^2 + H^\gamma, \tag{A1}$$

where

$$H^1 = \begin{pmatrix} H^f_{++} & 0 & H^f_{+-} & 0 \\ 0 & H^f_{++} & 0 & H^f_{+-} \\ H^f_{-+} & 0 & H^f_{--} & 0 \\ 0 & H^f_{-+} & 0 & H^f_{--} \end{pmatrix}, \quad H^2 = \begin{pmatrix} H^f_{++} & H^f_{+-} & 0 & 0 \\ H^f_{-+} & H^f_{--} & 0 & 0 \\ 0 & 0 & H^f_{++} & H^f_{+-} \\ 0 & 0 & H^f_{-+} & H^f_{--} \end{pmatrix},$$
$$H^\gamma = \begin{pmatrix} H^\gamma_{++++} & 0 & 0 & 0 \\ 0 & H^\gamma_{+-+-} & 0 & 0 \\ 0 & 0 & H^\gamma_{-+-+} & 0 \\ 0 & 0 & 0 & H^\gamma_{----} \end{pmatrix}, \tag{A2}$$

with $H^f_{\pm\pm}$ and $H^\gamma_{\pm\pm\pm\pm}$ given in Eq. (4.31).

Before antisymmetrizing the wave function in the artificial labels 1 and 2, we ignore the Pauli principle, and make the following ansatz for an energy eigenstate of two holes (distinguished by the labels 1 and 2):

$$\Psi^{ff}_{\sigma,m^1_+,m^1_-,m^2_+,m^2_-,m}(r_1,\chi_1,r_2,\chi_2,\gamma) = \begin{pmatrix} \psi_{\sigma,m^1_+,m^1_-,m^2_+,m^2_-,m,++}(r_1,r_2)\exp\left(i\sigma\left[m^1_+\chi_1 + m^2_+\chi_2 - \sigma_f\frac{\pi}{4}\right]\right)\exp[i\sigma(m-1)\gamma] \\ \sigma\sigma_f\psi_{\sigma,m^1_+,m^1_-,m^2_+,m^2_-,m,+-}(r_1,r_2)\exp(i\sigma[m^1_+\chi_1 + m^2_-\chi_2])\exp(i\sigma m\gamma) \\ \sigma\sigma_f\psi_{\sigma,m^1_+,m^1_-,m^2_+,m^2_-,m,-+}(r_1,r_2)\exp(i\sigma[m^1_-\chi_1 + m^2_+\chi_2])\exp(i\sigma m\gamma) \\ \psi_{\sigma,m^1_+,m^1_-,m^2_+,m^2_-,m,--}(r_1,r_2)\exp\left(i\sigma\left[m^1_-\chi_1 + m^2_-\chi_2 + \sigma_f\frac{\pi}{4}\right]\right)\exp[i\sigma(m+1)\gamma] \end{pmatrix}. \tag{A3}$$

As before, this solves the Schrödinger equation only if $m^i_- - m^i_+ = n+1$, $i = 1,2$. In this case, m is again an integer. The resulting radial Schrödinger equation now takes the form

$$H_r\psi_{\sigma,m^1_+,m^1_-,m^2_+,m^2_-,m}(r_1,r_2) = E_{\sigma,m^1_+,m^1_-,m^2_+,m^2_-,m}\psi_{\sigma,m^1_+,m^1_-,m^2_+,m^2_-,m}(r_1,r_2), \tag{A4}$$

with

$$\psi_{\sigma,m^1_+,m^1_-,m^2_+,m^2_-,m}(r_1,r_2) = \begin{pmatrix} \psi_{\sigma,m^1_+,m^1_-,m^2_+,m^2_-,m,++}(r_1,r_2) \\ \psi_{\sigma,m^1_+,m^1_-,m^2_+,m^2_-,m,+-}(r_1,r_2) \\ \psi_{\sigma,m^1_+,m^1_-,m^2_+,m^2_-,m,-+}(r_1,r_2) \\ \psi_{\sigma,m^1_+,m^1_-,m^2_+,m^2_-,m,--}(r_1,r_2) \end{pmatrix}. \tag{A5}$$

The radial Hamiltonian is given by

$$H_r = H^1_r + H^2_r + H^\gamma_r, \tag{A6}$$

with

$$H^1_r = \begin{pmatrix} H^1_{r++} & 0 & H^1_{r+-} & 0 \\ 0 & H^1_{r++} & 0 & H^1_{r+-} \\ H^1_{r-+} & 0 & H^1_{r--} & 0 \\ 0 & H^1_{r-+} & 0 & H^1_{r--} \end{pmatrix}, \quad H^2_r = \begin{pmatrix} H^2_{r++} & H^2_{r+-} & 0 & 0 \\ H^2_{r-+} & H^2_{r--} & 0 & 0 \\ 0 & 0 & H^2_{r++} & H^2_{r+-} \\ 0 & 0 & H^2_{r-+} & H^2_{r--} \end{pmatrix}, \tag{A7}$$

$$H^\gamma_r = \begin{pmatrix} H^\gamma_{r++++} & 0 & 0 & 0 \\ 0 & H^\gamma_{r+-+-} & 0 & 0 \\ 0 & 0 & H^\gamma_{r-+-+} & 0 \\ 0 & 0 & 0 & H^\gamma_{r----} \end{pmatrix}.$$

The matrix elements of the fermionic part of the radial Hamiltonian are given by

$$\begin{aligned} H^i_{r++} &= -\frac{1}{2M'}\left[\partial^2_{r_i} + \frac{1}{r_i}\partial_{r_i} - \frac{1}{r_i^2}\left(m^i_+ + \frac{n\rho^{2n}}{r_i^{2n}+\rho^{2n}}\right)^2\right], \\ H^i_{r+-} &= H^i_{r-+} = \sqrt{2}\Lambda\frac{nr_i^{n-1}\rho^n}{r_i^{2n}+\rho^{2n}}, \\ H^i_{r--} &= -\frac{1}{2M'}\left[\partial^2_{r_i} + \frac{1}{r_i}\partial_{r_i} - \frac{1}{r_i^2}\left(m^i_- - \frac{n\rho^{2n}}{r_i^{2n}+\rho^{2n}}\right)^2\right], \end{aligned} \tag{A8}$$

while the rotational skyrmion contributions are given by

$$\begin{aligned} H^\gamma_{r++++} &= \frac{n^2}{2\mathcal{D}(\rho)\rho^2}\left(m + \sigma n\frac{\Theta}{2\pi} - 1 - \frac{\rho^{2n}}{r_1^{2n}+\rho^{2n}} - \frac{\rho^{2n}}{r_2^{2n}+\rho^{2n}}\right)^2, \\ H^\gamma_{r+-+-} &= \frac{n^2}{2\mathcal{D}(\rho)\rho^2}\left(m + \sigma n\frac{\Theta}{2\pi} - \frac{\rho^{2n}}{r_1^{2n}+\rho^{2n}} + \frac{\rho^{2n}}{r_2^{2n}+\rho^{2n}}\right)^2, \\ H^\gamma_{r-+-+} &= \frac{n^2}{2\mathcal{D}(\rho)\rho^2}\left(m + \sigma n\frac{\Theta}{2\pi} + \frac{\rho^{2n}}{r_1^{2n}+\rho^{2n}} - \frac{\rho^{2n}}{r_2^{2n}+\rho^{2n}}\right)^2, \\ H^\gamma_{r----} &= \frac{n^2}{2\mathcal{D}(\rho)\rho^2}\left(m + \sigma n\frac{\Theta}{2\pi} + 1 + \frac{\rho^{2n}}{r_1^{2n}+\rho^{2n}} + \frac{\rho^{2n}}{r_2^{2n}+\rho^{2n}}\right)^2. \end{aligned} \tag{A9}$$

2. Symmetry properties of a pair of holes with the same flavor localized on a skyrmion

The spin operator I is again given by Eq. (4.39), such that

$$I\,\Psi^{ff}_{\sigma,m^1_+,m^1_-,m^2_+,m^2_-,m}(r_1,\chi_1,r_2,\chi_2,\gamma) = \left(m + \sigma n\frac{\Theta}{2\pi}\right)\Psi^{ff}_{\sigma,m^1_+,m^1_-,m^2_+,m^2_-,m}(r_1,\chi_1,r_2,\chi_2,\gamma). \quad \text{(A10)}$$

Since m is an integer, at least for $\Theta = 0$, the state with two holes of the same flavor localized on a skyrmion again has integer spin.

The symmetries D_i', O, and R act on the two-hole wave function

$$\Psi^{ff}_{\sigma,n}(r_1,\chi_1,r_2,\chi_2,\gamma) = \begin{pmatrix} \Psi^{ff}_{\sigma,n,++}(r_1,\chi_1,r_2,\chi_2,\gamma) \\ \Psi^{ff}_{\sigma,n,+-}(r_1,\chi_1,r_2,\chi_2,\gamma) \\ \Psi^{ff}_{\sigma,n,-+}(r_1,\chi_1,r_2,\chi_2,\gamma) \\ \Psi^{ff}_{\sigma,n,--}(r_1,\chi_1,r_2,\chi_2,\gamma) \end{pmatrix} \quad \text{(A11)}$$

as follows:

$$\begin{gathered} {}^{D_i'}\Psi^{ff}_{\sigma,n}(r_1,\chi_1,r_2,\chi_2,\gamma) = \exp\left(2ik_i^f a\right)\begin{pmatrix} \Psi^{ff}_{\sigma,n,--}(r_1,\chi_1,r_2,\chi_2,\gamma) \\ -\Psi^{ff}_{\sigma,n,-+}(r_1,\chi_1,r_2,\chi_2,\gamma) \\ -\Psi^{ff}_{\sigma,n,+-}(r_1,\chi_1,r_2,\chi_2,\gamma) \\ \Psi^{ff}_{\sigma,n,++}(r_1,\chi_1,r_2,\chi_2,\gamma) \end{pmatrix}, \\ {}^{O}\Psi^{ff}_{\sigma,n}(r_1,\chi_1,r_2,\chi_2,\gamma) = \begin{pmatrix} \Psi^{ff}_{\sigma,n,++}\left(r_1,\chi_1+\frac{\pi}{2},r_2,\chi_2+\frac{\pi}{2},\gamma-n\frac{\pi}{2}\right) \\ \sigma_f\Psi^{ff}_{\sigma,n,+-}\left(r_1,\chi_1+\frac{\pi}{2},r_2,\chi_2+\frac{\pi}{2},\gamma-n\frac{\pi}{2}\right) \\ \sigma_f\Psi^{ff}_{\sigma,n,-+}\left(r_1,\chi_1+\frac{\pi}{2},r_2,\chi_2+\frac{\pi}{2},\gamma-n\frac{\pi}{2}\right) \\ \Psi^{ff}_{\sigma,n,--}\left(r_1,\chi_1+\frac{\pi}{2},r_2,\chi_2+\frac{\pi}{2},\gamma-n\frac{\pi}{2}\right) \end{pmatrix}, \quad \text{(A12)} \\ {}^{R}\Psi^{ff}_{\sigma,n}(r_1,\chi_1,r_2,\chi_2,\gamma) = \begin{pmatrix} \Psi^{ff}_{\sigma,n,++}(r_1,-\chi_1,r_2,-\chi_2,-\gamma) \\ \Psi^{ff}_{\sigma,n,+-}(r_1,-\chi_1,r_2,-\chi_2,-\gamma) \\ \Psi^{ff}_{\sigma,n,-+}(r_1,-\chi_1,r_2,-\chi_2,-\gamma) \\ \Psi^{ff}_{\sigma,n,--}(r_1,-\chi_1,r_2,-\chi_2,-\gamma) \end{pmatrix}. \end{gathered}$$

For the two-hole energy eigenstates, this implies

$$\begin{aligned} {}^{D_i'}\Psi^{ff}_{\sigma,m^1_+,m^1_-,m^2_+,m^2_-,m}(r_1,\chi_1,r_2,\chi_2,\gamma) &= -\Psi^{ff}_{-\sigma,-m^1_-,-m^1_+,-m^2_-,-m^2_+,-m}(r_1,\chi_1,r_2,\chi_2,\gamma), \\ {}^{O}\Psi^{\alpha\alpha}_{\sigma,m^1_+,m^1_-,m^2_+,m^2_-,m}(r_1,\chi_1,r_2,\chi_2,\gamma) &= -\exp\left(i\sigma[m^1_+ + m^2_- - mn]\frac{\pi}{2}\right) \\ &\quad\times\Psi^{\beta\beta}_{\sigma,m^1_+,m^1_-,m^2_+,m^2_-,m}(r_1,\chi_1,r_2,\chi_2,\gamma), \\ {}^{O}\Psi^{\beta\beta}_{\sigma,m^1_+,m^1_-,m^2_+,m^2_-,m}(r_1,\chi_1,r_2,\chi_2,\gamma) &= \exp\left(i\sigma[m^1_+ + m^2_- - mn]\frac{\pi}{2}\right) \\ &\quad\times\Psi^{\alpha\alpha}_{\sigma,m^1_+,m^1_-,m^2_+,m^2_-,m}(r_1,\chi_1,r_2,\chi_2,\gamma), \\ {}^{R}\Psi^{\alpha\alpha}_{\sigma,m^1_+,m^1_-,m^2_+,m^2_-,m}(r_1,\chi_1,r_2,\chi_2,\gamma) &= \Psi^{\beta\beta}_{-\sigma,m^1_+,m^1_-,m^2_+,m^2_-,m}(r_1,\chi_1,r_2,\chi_2,\gamma), \\ {}^{R}\Psi^{\beta\beta}_{\sigma,m^1_+,m^1_-,m^2_+,m^2_-,m}(r_1,\chi_1,r_2,\chi_2,\gamma) &= \Psi^{\alpha\alpha}_{-\sigma,m^1_+,m^1_-,m^2_+,m^2_-,m}(r_1,\chi_1,r_2,\chi_2,\gamma). \end{aligned} \quad \text{(A13)}$$

Here, we have again assumed an appropriate phase convention for the radial wave function $\psi_{\sigma,m^1_+,m^1_-,m^2_+,m^2_-,m}(r_1,r_2)$. In the context of the shift symmetries D_i', we have used

$$\begin{aligned} \psi_{\sigma,m^1_+,m^1_-,m^2_+,m^2_-,m,--}(r_1,r_2) &= \psi_{-\sigma,-m^1_-,-m^1_+,-m^2_-,-m^2_+,-m,++}(r_1,r_2), \\ \psi_{\sigma,m^1_+,m^1_-,m^2_+,m^2_-,m,-+}(r_1,r_2) &= \psi_{-\sigma,-m^1_-,-m^1_+,-m^2_-,-m^2_+,-m,+-}(r_1,r_2), \\ \psi_{\sigma,m^1_+,m^1_-,m^2_+,m^2_-,m,+-}(r_1,r_2) &= \psi_{-\sigma,-m^1_-,-m^1_+,-m^2_-,-m^2_+,-m,-+}(r_1,r_2), \\ \psi_{\sigma,m^1_+,m^1_-,m^2_+,m^2_-,m,++}(r_1,r_2) &= \psi_{-\sigma,-m^1_-,-m^1_+,-m^2_-,-m^2_+,-m,--}(r_1,r_2). \end{aligned} \quad \text{(A14)}$$

These relations follow from the symmetries of the radial Schrödinger equation (A4). In the context of the reflection symmetry R, we have used

$$\begin{aligned}
\psi_{\sigma,m_+^1,m_-^1,m_+^2,m_-^2,m,++}(r_1,r_2) &= \psi_{-\sigma,m_+^1,m_-^1,m_+^2,m_-^2,m,++}(r_1,r_2),\\
\psi_{\sigma,m_+^1,m_-^1,m_+^2,m_-^2,m,+-}(r_1,r_2) &= \psi_{-\sigma,m_+^1,m_-^1,m_+^2,m_-^2,m,+-}(r_1,r_2),\\
\psi_{\sigma,m_+^1,m_-^1,m_+^2,m_-^2,m,-+}(r_1,r_2) &= \psi_{-\sigma,m_+^1,m_-^1,m_+^2,m_-^2,m,-+}(r_1,r_2),\\
\psi_{\sigma,m_+^1,m_-^1,m_+^2,m_-^2,m,--}(r_1,r_2) &= \psi_{-\sigma,m_+^1,m_-^1,m_+^2,m_-^2,m,--}(r_1,r_2).
\end{aligned} \tag{A15}$$

The relations in Eq. (A15) follow from the symmetries of the radial Schrödinger equation (A4) for $\Theta = 0$. As before, for $\Theta \neq 0$ or π, the Hopf term explicitly breaks the reflection symmetry.

Let us now impose the Pauli principle by explicitly antisymmetrizing the wave function in the artificial indices 1 and 2. For this purpose, we act with the pair permutation P, i.e.,

$${}^P\Psi^{ff}_{\sigma,n}(r_1,\chi_1,r_2,\chi_2,\gamma) = \begin{pmatrix} \Psi^{ff}_{\sigma,n,++}(r_2,\chi_2,r_1,\chi_1,\gamma)\\ \Psi^{ff}_{\sigma,n,-+}(r_2,\chi_2,r_1,\chi_1,\gamma)\\ \Psi^{ff}_{\sigma,n,+-}(r_2,\chi_2,r_1,\chi_1,\gamma)\\ \Psi^{ff}_{\sigma,n,--}(r_2,\chi_2,r_1,\chi_1,\gamma)\end{pmatrix}. \tag{A16}$$

For an energy eigenstate, this implies

$${}^P\Psi^{ff}_{\sigma,m_+^1,m_-^1,m_+^2,m_-^2,m}(r_1,\chi_1,r_2,\chi_2,\gamma) = \Psi^{ff}_{\sigma,m_+^2,m_-^2,m_+^1,m_-^1,m}(r_1,\chi_1,r_2,\chi_2,\gamma). \tag{A17}$$

Here, we have assumed a symmetric radial wave function, i.e.,

$$\begin{aligned}
\psi_{\sigma,m_+^1,m_-^1,m_+^2,m_-^2,m,++}(r_2,r_1) &= \psi_{\sigma,m_+^2,m_-^2,m_+^1,m_-^1,m,++}(r_1,r_2),\\
\psi_{\sigma,m_+^1,m_-^1,m_+^2,m_-^2,m,-+}(r_2,r_1) &= \psi_{\sigma,m_+^2,m_-^2,m_+^1,m_-^1,m,+-}(r_1,r_2),\\
\psi_{\sigma,m_+^1,m_-^1,m_+^2,m_-^2,m,+-}(r_2,r_1) &= \psi_{\sigma,m_+^2,m_-^2,m_+^1,m_-^1,m,-+}(r_1,r_2),\\
\psi_{\sigma,m_+^1,m_-^1,m_+^2,m_-^2,m,--}(r_2,r_1) &= \psi_{\sigma,m_+^2,m_-^2,m_+^1,m_-^1,m,--}(r_1,r_2).
\end{aligned} \tag{A18}$$

The properly antisymmetrized wave function now takes the form

$$\widetilde{\Psi}^{ff}_{\sigma,n}(r_1,\chi_1,r_2,\chi_2,\gamma) = \frac{1}{\sqrt{2}}\left[\Psi^{ff}_{\sigma,n}(r_1,\chi_1,r_2,\chi_2,\gamma) - {}^P\,\Psi^{ff}_{\sigma,n}(r_1,\chi_1,r_2,\chi_2,\gamma)\right]. \tag{A19}$$

For an energy eigenstate, this implies

$$\begin{aligned}
&\widetilde{\Psi}^{ff}_{\sigma,m_+^1,m_-^1,m_+^2,m_-^2,m}(r_1,\chi_1,r_2,\chi_2,\gamma)\\
&= \frac{1}{\sqrt{2}}\left[\Psi^{ff}_{\sigma,m_+^1,m_-^1,m_+^2,m_-^2,m}(r_1,\chi_1,r_2,\chi_2,\gamma) - \Psi^{ff}_{\sigma,m_+^2,m_-^2,m_+^1,m_-^1,m}(r_1,\chi_1,r_2,\chi_2,\gamma)\right].
\end{aligned} \tag{A20}$$

As expected, in order to obtain a nonvanishing wave function, the two sets of quantum numbers m_+^1, m_-^1 and m_+^2, m_-^2 must be different because otherwise two identical fermions would occupy the same single-particle state. If one would consider an antisymmetric radial wave function, one could allow $m_+^1 = m_+^2$ and $m_-^1 = m_-^2$.

Based on Eq. (A13), the properly antisymmetrized two-hole energy eigenstates transform as follows:

$$\begin{aligned}
{}^{D_i'}\widetilde{\Psi}^{ff}_{\sigma,m_+^1,m_-^1,m_+^2,m_-^2,m}(r_1,\chi_1,r_2,\chi_2,\gamma) &= -\widetilde{\Psi}^{ff}_{-\sigma,-m_-^1,-m_+^1,-m_-^2,-m_+^2,-m}(r_1,\chi_1,r_2,\chi_2,\gamma),\\
{}^{O}\widetilde{\Psi}^{\alpha\alpha}_{\sigma,m_+^1,m_-^1,m_+^2,m_-^2,m}(r_1,\chi_1,r_2,\chi_2,\gamma) &= -\exp\left(i\sigma[m_+^1 + m_-^2 - mn]\frac{\pi}{2}\right)\\
&\quad\times \widetilde{\Psi}^{\beta\beta}_{\sigma,m_+^1,m_-^1,m_+^2,m_-^2,m}(r_1,\chi_1,r_2,\chi_2,\gamma),\\
{}^{O}\widetilde{\Psi}^{\beta\beta}_{\sigma,m_+^1,m_-^1,m_+^2,m_-^2,m}(r_1,\chi_1,r_2,\chi_2,\gamma) &= \exp\left(i\sigma[m_+^1 + m_-^2 - mn]\frac{\pi}{2}\right)\\
&\quad\times \widetilde{\Psi}^{\alpha\alpha}_{\sigma,m_+^1,m_-^1,m_+^2,m_-^2,m}(r_1,\chi_1,r_2,\chi_2,\gamma),\\
{}^{R}\widetilde{\Psi}^{\alpha\alpha}_{\sigma,m_+^1,m_-^1,m_+^2,m_-^2,m}(r_1,\chi_1,r_2,\chi_2,\gamma) &= \widetilde{\Psi}^{\beta\beta}_{-\sigma,m_+^1,m_-^1,m_+^2,m_-^2,m}(r_1,\chi_1,r_2,\chi_2,\gamma),\\
{}^{R}\widetilde{\Psi}^{\beta\beta}_{\sigma,m_+^1,m_-^1,m_+^2,m_-^2,m}(r_1,\chi_1,r_2,\chi_2,\gamma) &= \widetilde{\Psi}^{\alpha\alpha}_{-\sigma,m_+^1,m_-^1,m_+^2,m_-^2,m}(r_1,\chi_1,r_2,\chi_2,\gamma).
\end{aligned} \tag{A21}$$

In order to show this for the rotation O, we have used $m_+^1 + m_-^2 = m_+^2 + m_-^1$.

Finally, let us combine states with flavors $\alpha\alpha$ and $\beta\beta$ to eigenstates of O:

$$\widetilde{\Psi}^{\pm}_{\sigma,m^1_+,m^1_-,m^2_+,m^2_-,m}(r_1,\chi_1,r_2,\chi_2,\gamma) = \frac{1}{\sqrt{2}}\big[\widetilde{\Psi}^{\alpha\alpha}_{\sigma,m^1_+,m^1_-,m^2_+,m^2_-,m}(r_1,\chi_1,r_2,\chi_2,\gamma) \pm i\,\widetilde{\Psi}^{\beta\beta}_{\sigma,m^1_+,m^1_-,m^2_+,m^2_-,m}(r_1,\chi_1,r_2,\chi_2,\gamma)\big], \tag{A22}$$

which transform as

$$\begin{aligned}
{}^{D_i'}\widetilde{\Psi}^{\pm}_{\sigma,m^1_+,m^1_-,m^2_+,m^2_-,m}(r_1,\chi_1,r_2,\chi_2,\gamma) &= -\widetilde{\Psi}^{\pm}_{-\sigma,-m^1_-,-m^1_+,-m^2_-,-m^2_+,-m}(r_1,\chi_1,r_2,\chi_2,\gamma),\\
{}^{O}\widetilde{\Psi}^{\pm}_{\sigma,m^1_+,m^1_-,m^2_+,m^2_-,m}(r_1,\chi_1,r_2,\chi_2,\gamma) &= \pm i \exp\left(i\sigma[m^1_+ + m^2_- - mn]\frac{\pi}{2}\right)\\
&\quad\times \widetilde{\Psi}^{\pm}_{\sigma,m^1_+,m^1_-,m^2_+,m^2_-,m}(r_1,\chi_1,r_2,\chi_2,\gamma),\\
{}^{R}\widetilde{\Psi}^{\pm}_{\sigma,m^1_+,m^1_-,m^2_+,m^2_-,m}(r_1,\chi_1,r_2,\chi_2,\gamma) &= \pm i\,\widetilde{\Psi}^{\mp}_{-\sigma,m^1_+,m^1_-,m^2_+,m^2_-,m}(r_1,\chi_1,r_2,\chi_2,\gamma).
\end{aligned} \tag{A23}$$

The lowest-energy states in the same flavor channel are expected to correspond to $m^1_+ = -1$, $m^1_- = 1$, $m^2_+ = -2$, $m^2_- = 0$, $m = 0$ or $m^1_+ = -1$, $m^1_- = 1$, $m^2_+ = 0$, $m^2_- = 2$, $m = 0$. These states transform as

$$\begin{aligned}
{}^{D_i'}\widetilde{\Psi}^{\pm}_{\sigma,-1,1,-2,0,0}(r_1,\chi_1,r_2,\chi_2,\gamma) &= -\widetilde{\Psi}^{\pm}_{-\sigma,-1,1,0,2,0}(r_1,\chi_1,r_2,\chi_2,\gamma),\\
{}^{O}\widetilde{\Psi}^{\pm}_{\sigma,-1,1,-2,0,0}(r_1,\chi_1,r_2,\chi_2,\gamma) &= \pm\sigma\,\widetilde{\Psi}^{\pm}_{\sigma,-1,1,-2,0,0}(r_1,\chi_1,r_2,\chi_2,\gamma),\\
{}^{R}\widetilde{\Psi}^{\pm}_{\sigma,-1,1,-2,0,0}(r_1,\chi_1,r_2,\chi_2,\gamma) &= \pm i\,\widetilde{\Psi}^{\mp}_{-\sigma,-1,1,-2,0,0}(r_1,\chi_1,r_2,\chi_2,\gamma),\\
{}^{D_i'}\widetilde{\Psi}^{\pm}_{\sigma,-1,1,0,2,0}(r_1,\chi_1,r_2,\chi_2,\gamma) &= -\widetilde{\Psi}^{\pm}_{-\sigma,-1,1,-2,0,0}(r_1,\chi_1,r_2,\chi_2,\gamma),\\
{}^{O}\widetilde{\Psi}^{\pm}_{\sigma,-1,1,0,2,0}(r_1,\chi_1,r_2,\chi_2,\gamma) &= \mp\sigma\,\widetilde{\Psi}^{\pm}_{\sigma,-1,1,0,2,0}(r_1,\chi_1,r_2,\chi_2,\gamma),\\
{}^{R}\widetilde{\Psi}^{\pm}_{\sigma,-1,1,0,2,0}(r_1,\chi_1,r_2,\chi_2,\gamma) &= \pm i\,\widetilde{\Psi}^{\mp}_{-\sigma,-1,1,0,2,0}(r_1,\chi_1,r_2,\chi_2,\gamma).
\end{aligned} \tag{A24}$$

This implies that the states $\widetilde{\Psi}^{+}_{+,-1,1,-2,0,0}(r_1,\chi_1,r_2,\chi_2,\gamma)$, $\widetilde{\Psi}^{-}_{-,-1,1,-2,0,0}(r_1,\chi_1,r_2,\chi_2,\gamma)$, $\widetilde{\Psi}^{+}_{-,-1,1,0,2,0}(r_1,\chi_1,r_2,\chi_2,\gamma)$, $\widetilde{\Psi}^{-}_{+,-1,1,0,2,0}(r_1,\chi_1,r_2,\chi_2,\gamma)$ are s waves, while the states $\widetilde{\Psi}^{+}_{+,-1,1,0,2,0}(r_1,\chi_1,r_2,\chi_2,\gamma)$, $\widetilde{\Psi}^{-}_{-,-1,1,0,2,0}(r_1,\chi_1,r_2,\chi_2,\gamma)$, $\widetilde{\Psi}^{+}_{-,-1,1,-2,0,0}(r_1,\chi_1,r_2,\chi_2,\gamma)$, $\widetilde{\Psi}^{-}_{+,-1,1,-2,0,0}(r_1,\chi_1,r_2,\chi_2,\gamma)$ are d waves.

3. Comparison with magnon-mediated two-hole bound states of the same flavor

In Ref. 14, states of two holes of the same flavor bound by one-magnon exchange have also been investigated. Here, we summarize as well as extend some of the relevant results. We consider two holes of the same flavor f with opposite spins $+$ and $-$. In the rest frame, the wave function depends on the distance vector $\vec{r}$ which points from the spin $+$ hole to the spin $-$ hole. Since magnon exchange is accompanied by a spin flip, the vector $\vec{r}$ changes its direction in the magnon exchange process. The Schrödinger equation thus takes the form

$$-\frac{1}{M'}\Delta\Psi(\vec{r}) + V^{ff}(\vec{r})\Psi(-\vec{r}) = E\Psi(\vec{r}). \tag{A25}$$

The one-magnon exchange potential for two holes of the same flavor is given by

$$V^{\alpha\alpha}(\vec{r}) = \frac{\Lambda^2}{2\pi\rho_s}\frac{\sin(2\varphi)}{r^2}, \quad V^{\beta\beta}(\vec{r}) = -\frac{\Lambda^2}{2\pi\rho_s}\frac{\sin(2\varphi)}{r^2}. \tag{A26}$$

We make a separation ansatz

$$\Psi(\vec{r}) = R'(r)\chi'(\varphi). \tag{A27}$$

The ground state is even with respect to the reflection of $\vec{r}$ to $-\vec{r}$, i.e.,

$$\chi'^1(\varphi+\pi) = \chi'^1(\varphi). \tag{A28}$$

The angular part of the Schrödinger equation then takes the form

$$-\frac{d^2\chi'^1_\pm(\varphi)}{d\varphi^2} \pm \frac{M'\Lambda^2}{2\pi\rho_s}\sin(2\varphi)\chi'^1_\pm(\varphi) = -\lambda_1\chi'^1_\pm(\varphi). \tag{A29}$$

Here, $+$ and $-$ are associated with an $\alpha\alpha$ and a $\beta\beta$ pair, respectively. Again, Eq. (A29) is a Mathieu equation. The ground state with eigenvalue $-\lambda_1$ takes the form

$$\begin{aligned}
\chi'^1_\pm(\varphi) &= \chi^1_\pm\left(\varphi - \frac{\pi}{4}\right) = \frac{1}{\sqrt{\pi}}\mathrm{ce}_0\left(\varphi - \frac{\pi}{4}, \pm\frac{M'\Lambda^2}{4\pi\rho_s}\right),\\
\lambda_1 &= \frac{1}{2}\left(\frac{M'\Lambda^2}{4\pi\rho_s}\right)^2 + \mathcal{O}(\Lambda^8).
\end{aligned} \tag{A30}$$

The first excited states are odd with respect to the reflection of $\vec{r}$ to $-\vec{r}$, i.e.,

$$\chi'^2_\pm(\varphi+\pi) = -\chi'^2_\pm(\varphi), \tag{A31}$$

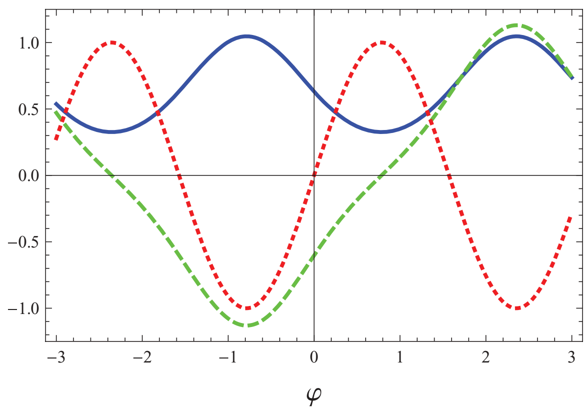

FIG. 5. (Color online) Angular wave functions $\mathrm{ce}_0(\varphi - \frac{\pi}{4}, \frac{1}{2}M'\gamma)$ (solid curve) and $\mathrm{se}_1(\varphi - \frac{\pi}{4}, \frac{1}{2}M'\gamma)$ (dashed curve) as well as angle dependence $\sin(2\varphi)$ of the potential (dotted curve) for two holes of flavor α residing in a circular hole pocket ($M'\Lambda^2/4\pi\rho_s = 1.25$).

and the angular part of the Schrödinger equation now reads as

$$-\frac{d^2\chi_{\mp}^{\prime 2}(\varphi)}{d\varphi^2} \mp \frac{M'\Lambda^2}{2\pi\rho_s}\sin(2\varphi)\chi_{\mp}^{\prime 2}(\varphi) = -\lambda_2\chi_{\mp}^{\prime 2}(\varphi). \quad \text{(A32)}$$

Now, $-$ and $+$ are associated with an $\alpha\alpha$ and a $\beta\beta$ pair, respectively. The excited states with eigenvalue $-\lambda_2$ are given by

$$\chi_{+}^{\prime 2}(\varphi) = \chi_{+}^{2}\left(\varphi - \frac{\pi}{4}\right) = \frac{1}{\sqrt{\pi}}\mathrm{se}_1\left(\varphi - \frac{\pi}{4}, \frac{M'\Lambda^2}{4\pi\rho_s}\right),$$
$$\chi_{-}^{\prime 2}(\varphi) = \chi_{-}^{2}\left(\varphi - \frac{\pi}{4}\right) = -\frac{1}{\sqrt{\pi}}\mathrm{ce}_1\left(\varphi - \frac{\pi}{4}, -\frac{M'\Lambda^2}{4\pi\rho_s}\right),$$
$$\lambda_2 = -1 + \frac{M'\Lambda^2}{4\pi\rho_s} + \frac{1}{8}\left(\frac{M'\Lambda^2}{4\pi\rho_s}\right)^2 - \frac{1}{64}\left(\frac{M'\Lambda^2}{4\pi\rho_s}\right)^3 + \mathcal{O}(\Lambda^8). \quad \text{(A33)}$$

The angular wave functions for the ground state and for the first excited state together with the angular dependence of the one-magnon exchange potential are shown in Fig. 5.

As before, the radial Schrödinger equation takes the form of Eq. (4.53). Again, the short-distance repulsion between two holes is modeled by a hard core of radius r_0', i.e., $R'(r_0') = 0$. The value of r_0' may, however, differ from r_0 in the $\alpha\beta$ case. The radial wave functions are thus given by

$$R_i'(r) = A_i' K_\nu(\sqrt{M'|E_{ik}'|}r), \quad k = 1,2,3,\ldots, \quad \nu = i\sqrt{\lambda_i} \quad \text{(A34)}$$

and the energy is determined from $K_\nu(\sqrt{M'|E_{ik}'|}r_0') = 0$.

There are two degenerate states, one for an $\alpha\alpha$ and one for a $\beta\beta$ pair, which are eigenstates of flavor related to each other by a 90° rotation. The two degenerate states can be combined to eigenstates of the rotation symmetry O. For this purpose, we construct the two-component wave functions

$$\Psi_{\pm}^{\prime 1}(\vec{r}) = R_1'(r)\begin{pmatrix}\chi_{+}^{\prime 1}(\varphi)\\ \pm i\chi_{-}^{\prime 1}(\varphi)\end{pmatrix}, \quad \Psi_{\pm}^{\prime 2}(\vec{r}) = R_2'(r)\begin{pmatrix}\chi_{-}^{\prime 2}(\varphi)\\ \pm\chi_{+}^{\prime 2}(\varphi)\end{pmatrix}, \quad \text{(A35)}$$

the first component of which represents the $\alpha\alpha$ and the second component of which represents the $\beta\beta$ pair. Under the various

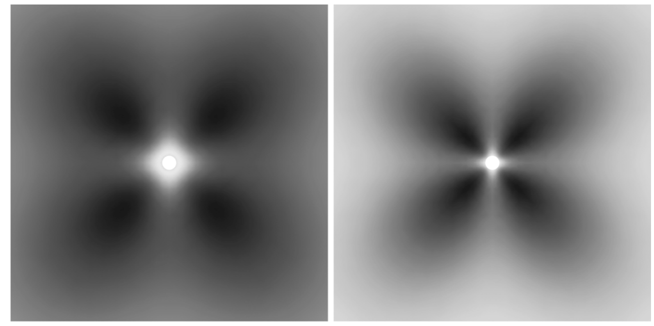

FIG. 6. Probability distribution for bound states of two holes with flavors $\alpha\alpha$ or $\beta\beta$, combined to an eigenstate of the 90° rotation symmetry O. Left panel: the ground state with p-wave symmetry. Right panel: excited states with s- or d-wave symmetry, but with identical probability densities ($M'\Lambda^2/4\pi\rho_s = 1.25$, $r_0' = a$).

symmetries, the two degenerate ground states transform as

$$\begin{aligned}
{}^{D_i'}\Psi_{\pm}^{\prime 1}(\vec{r}) &= R_1'(r)\begin{pmatrix}\chi_{+}^{\prime 1}(\varphi+\pi)\\ \pm i\chi_{-}^{\prime 1}(\varphi+\pi)\end{pmatrix}\\
&= R_1'(r)\begin{pmatrix}\chi_{+}^{\prime 1}(\varphi)\\ \pm i\chi_{-}^{\prime 1}(\varphi)\end{pmatrix} = \Psi_{\pm}^{\prime 1}(\vec{r}),\\
{}^{O}\Psi_{\pm}^{\prime 1}(\vec{r}) &= R_1'(r)\begin{pmatrix}\pm i\chi_{-}^{\prime 1}(\varphi+\frac{\pi}{2})\\ -\chi_{+}^{\prime 1}(\varphi+\frac{\pi}{2})\end{pmatrix}\\
&= R_1'(r)\begin{pmatrix}\pm i\chi_{+}^{\prime 1}(\varphi)\\ -\chi_{-}^{\prime 1}(\varphi)\end{pmatrix} = \pm i\Psi_{\pm}^{\prime 1}(\vec{r}),\\
{}^{R}\Psi_{\pm}^{\prime 1}(\vec{r}) &= R_1'(r)\begin{pmatrix}\pm i\chi_{-}^{\prime 1}(-\varphi)\\ \chi_{+}^{\prime 1}(-\varphi)\end{pmatrix}\\
&= R_1'(r)\begin{pmatrix}\pm i\chi_{+}^{\prime 1}(\varphi)\\ \chi_{-}^{\prime 1}(\varphi)\end{pmatrix} = \pm i\Psi_{\mp}^{\prime 1}(\vec{r}).
\end{aligned} \quad \text{(A36)}$$

Again, the corresponding eigenvalues of the 90° rotation O are $o = \pm i$, and hence, as for $\alpha\beta$ pairs, the symmetry is actually p wave. Similarly, the two degenerate first excited states transform as

$$\begin{aligned}
{}^{D_i'}\Psi_{\pm}^{\prime 2}(\vec{r}) &= -R_2'(r)\begin{pmatrix}\chi_{-}^{\prime 2}(\varphi)\\ \pm\chi_{+}^{\prime 2}(\varphi)\end{pmatrix} = -\Psi_{\pm}^{\prime 2}(\vec{r}),\\
{}^{O}\Psi_{\pm}^{\prime 2}(\vec{r}) &= R_2'(r)\begin{pmatrix}\pm\chi_{+}^{\prime 2}(\varphi+\frac{\pi}{2})\\ -\chi_{-}^{\prime 2}(\varphi+\frac{\pi}{2})\end{pmatrix}\\
&= R_2'(r)\begin{pmatrix}\mp\chi_{-}^{\prime 2}(\varphi)\\ -\chi_{+}^{\prime 2}(\varphi)\end{pmatrix} = \mp\Psi_{\pm}^{\prime 2}(\vec{r}),\\
{}^{R}\Psi_{\pm}^{\prime 2}(\vec{r}) &= R_2'(r)\begin{pmatrix}\pm\chi_{+}^{\prime 2}(-\varphi)\\ \chi_{-}^{\prime 2}(-\varphi)\end{pmatrix}\\
&= R_2'(r)\begin{pmatrix}\pm\chi_{-}^{\prime 2}(\varphi)\\ \chi_{+}^{\prime 2}(\varphi)\end{pmatrix} = \pm\Psi_{\pm}^{\prime 2}(\vec{r}).
\end{aligned} \quad \text{(A37)}$$

Again, the first excited states transform as s or d waves. The resulting probability distributions, which resemble d_{xy} symmetry, are illustrated in Fig. 6 for the ground state (left panel) and the first excited state (right panel). Unlike for an $\alpha\beta$ pair, in the same flavor case, the lowest-energy bound states localized on a skyrmion have a different transformation behavior than the magnon-mediated two-hole bound states.

*fjjiang@ntnu.edu.tw

[1] U.-J. Wiese and H.-P. Ying, Z. Phys. B: Condens. Matter **93**, 147 (1994).
[2] B. B. Beard and U.-J. Wiese, Phys. Rev. Lett. **77**, 5130 (1996).
[3] A. W. Sandvik and H.-G. Evertz, Phys. Rev. B **82**, 024407 (2010).
[4] F.-J. Jiang and U.-J. Wiese, Phys. Rev. B **83**, 155120 (2011).
[5] H. G. Evertz, G. Lana, and M. Marcu, Phys. Rev. Lett. **70**, 875 (1993).
[6] M. Brunner, F. F. Assaad, and A. Muramatsu, Phys. Rev. B **62**, 15480 (2000).
[7] A. S. Mishchenko, N. V. Prokof'ev, and B. V. Svistunov, Phys. Rev. B **64**, 033101 (2001).
[8] S. Chakravarty, B. I. Halperin, and D. R. Nelson, Phys. Rev. B **39**, 2344 (1989).
[9] H. Neuberger and T. Ziman, Phys. Rev. B **39**, 2608 (1989).
[10] D. S. Fisher, Phys. Rev. B **39**, 11783 (1989).
[11] P. Hasenfratz and H. Leutwyler, Nucl. Phys. B **343**, 241 (1990).
[12] J. Gasser and H. Leutwyler, Nucl. Phys. B **250**, 465 (1985).
[13] F. Kämpfer, M. Moser, and U.-J. Wiese, Nucl. Phys. B **729**, 317 (2005).
[14] C. Brügger, F. Kämpfer, M. Moser, M. Pepe, and U.-J. Wiese, Phys. Rev. B **74**, 224432 (2006).
[15] J. Gasser, M. E. Sainio, and A. Svarc, Nucl. Phys. B **307**, 779 (1988).
[16] E. Jenkins and A. Manohar, Phys. Lett. B **255**, 558 (1991).
[17] V. Bernard, N. Kaiser, J. Kambor, and U.-G. Meissner, Nucl. Phys. B **388**, 315 (1992).
[18] T. Becher and H. Leutwyler, Eur. Phys. J. C **9**, 643 (1999).
[19] B. I. Shraiman and E. D. Siggia, Phys. Rev. Lett. **60**, 740 (1988); **61**, 467 (1988); **62**, 1564 (1989); Phys. Rev. B **46**, 8305 (1992).
[20] X. G. Wen, Phys. Rev. B **39**, 7223 (1989).
[21] R. Shankar, Phys. Rev. Lett. **63**, 203 (1989); Nucl. Phys. B **330**, 433 (1990).
[22] C. Kübert and A. Muramatsu, Phys. Rev. B **47**, 787 (1993).
[23] M. Y. Kuchiev and O. P. Sushkov, Phys. C (Amsterdam) **218**, 197 (1993).
[24] C. Brügger, F. Kämpfer, M. Pepe, and U.-J. Wiese, Eur. Phys. J. B **53**, 433 (2006).
[25] C. Brügger, C. P. Hofmann, F. Kämpfer, M. Pepe, and U.-J. Wiese, Phys. Rev. B **75**, 014421 (2007).
[26] O. P. Sushkov and V. N. Kotov, Phys. Rev. B **70**, 024503 (2004).
[27] V. N. Kotov and O. P. Sushkov, Phys. Rev. B **72**, 184519 (2005).
[28] F. Kämpfer, B. Bessire, M. Wirz, C. P. Hofmann, F.-J. Jiang, and U.-J. Wiese, Phys. Rev. B **85**, 075123 (2012).
[29] F.-J. Jiang, F. Kämpfer, C. P. Hofmann, and U.-J. Wiese, Eur. Phys. J. B **69**, 473 (2009).
[30] C. Brügger, C. P. Hofmann, F. Kämpfer, M. Moser, M. Pepe, and U.-J. Wiese, Phys. Rev. B **75**, 214405 (2007).
[31] F. D. M. Haldane, Phys. Rev. Lett. **61**, 1029 (1988).
[32] N. Read and S. Sachdev, Phys. Rev. Lett. **62**, 1694 (1989); Nucl. Phys. B **316**, 609 (1989).
[33] B. I. Shraiman and E. D. Siggia, Phys. Rev. B **42**, 2485 (1990).
[34] R. J. Gooding, Phys. Rev. Lett. **66**, 2266 (1991).
[35] R. J. Gooding and A. Mailhot, Phys. Rev. B **48**, 6132 (1993).
[36] S. Haas, F.-C. Zhang, F. Mila, and T. M. Rice, Phys. Rev. Lett. **77**, 3021 (1996).
[37] E. C. Marino and M. B. Silva Neto, Phys. Rev. B **64**, 092511 (2001).
[38] O. I. Motrunich and A. Vishwanath, Phys. Rev. B **70**, 075104 (2004).
[39] T. Senthil, A. Vishwanath, L. Balents, S. Sachdev, and M. P. A. Fisher, Science **303**, 1490 (2004); T. Senthil, L. Balents, S. Sachdev, A. Vishwanath, and M. P. A. Fisher, Phys. Rev. B **70**, 144407 (2004).
[40] O. Bär, M. Imboden, and U.-J. Wiese, Nucl. Phys. B **686**, 347 (2004).
[41] U.-J. Wiese, Nucl. Phys. Proc. Suppl. **141**, 143 (2005).
[42] T. Morinari, Phys. Rev. B **72**, 104502 (2005).
[43] L. Fu, S. Sachdev, and C. Xu, Phys. Rev. B **83**, 165123 (2011).
[44] I. Raicevic, D. Popovic, C. Panagopoulos, L. Benfatto, M. B. Silva Neto, E. S. Choi, and T. Sasagawa, Phys. Rev. Lett. **106**, 227206 (2011).
[45] G. Baskaran, arXiv:1108.3562.
[46] J. A. Vergés, E. Louis, P. S. Lomdahl, F. Guinea, and A. R. Bishop, Phys. Rev. B **43**, 6099 (1991).
[47] G. Seibold, Phys. Rev. B **58**, 15520 (1998).
[48] M. Berciu and S. John, Phys. Rev. B **59**, 15143 (1999).
[49] C. Timm and K. H. Bennemann, Phys. Rev. Lett. **84**, 4994 (2000).
[50] T. H. R. Skyrme, Proc. R. Soc. Lond. A **260**, 127 (1961); Nucl. Phys. **31**, 556 (1962).
[51] A. A. Belavin and A. M. Polyakov, Pis'ma Zh. Éksp. Teor. Fiz. **22**, 503 (1975) [JETP Lett. **22**, 245 (1975)].
[52] G. S. Adkins, C. R. Nappi, and E. Witten, Nucl. Phys. B **228**, 552 (1983).
[53] J. Goldstone and F. Wilczek, Phys. Rev. Lett. **47**, 986 (1981).
[54] O. Bär and U. J. Wiese, Nucl. Phys. B **609**, 225 (2001).
[55] F. Wilczek and A. Zee, Phys. Rev. Lett. **51**, 2250 (1983).
[56] X. G. Wen and A. Zee, Phys. Rev. Lett. **61**, 1025 (1988).
[57] T. Dombre and N. Read, Phys. Rev. B **38**, 7181 (1988).
[58] E. Fradkin and M. Stone, Phys. Rev. B **38**, 7215 (1988).
[59] V. A. Fateev, I. V. Frolov, and A. S. Schwarz, Yad. Fiz. **30**, 1134 (1979) [Sov. J. Nucl. Phys. **30**, 590 (1979)].
[60] B. Berg and M. Lüscher, Commun. Math. Phys. **69**, 57 (1979).
[61] R. Tycko, S. E. Barrett, G. Dabbagh, L. N. Pfeiffer, and K. W. West, Science **268**, 1460 (1995).
[62] S. E. Barrett, G. Dabbagh, L. N. Pfeiffer, K. W. West, and R. Tycko, Phys. Rev. Lett. **74**, 5112 (1995).
[63] S. M. Girvin, *The Quantum Hall Effect: Novel Excitations and Broken Symmetries, Topological Aspects of Low Dimensional Systems*, edited by A. Comtet, T. Jolicoeur, S. Ouvry, and F. David (Springer-Verlag, Berlin and Les Editions de Physique, Les Ulis, 2000).
[64] M. Abramowitz and I. A. Stegun, *Handbook of Mathematical Functions* (Dover, New York, 1972).